Only two samples; 95SLC20R and 95SCB08R, are shown in Fig. 5–5–5, and the rest of samples are plotted in the same range as these two.

- Group B: Patterns show the gentle slope between La and Sm, and descend to the left (depleted in light–REE)

5 samples: 95SFPG02R, 95SFPG03R, 95SCB03R1,R2, 95SCB06R

Three samples (95SFPG03R, 95SCB03R2 and 95SCB06R) are plotted in Fig. 5–5–5. All five samples show a similar pattern but they have the different concentration of each element. The samples of this group have no common geological features and the reason for this variation of the concentration is unknown. 95SFPG03R, which occupies the lowest side of the Fig 5–5–5, was collected on the knoll closest to the island arc (the Tonga islands).

- Group C: Pattern shows the gentle slope between La and Sm and almost flat line

1 sample: 95SEPG01R

This sample was collected on the knoll west of the spreading center and has the different geological environment from those of other samples.

Except for one sample of Group C, the variations of chondrite normalized pattern are not related to the geological and petrological features. The glass part of the child margin (R2 and CN at the end of sample number) and the inner part of the same body (R1 and R at the end of the sample number) shows no differences in chondrite normalized pattern.

As mentioned above, the chemical composition suggests that the basalt produced by the volcanic activities of the spreading center in the Lau basin belong to tholeiitic series and they have chemical characters both of the island arc tholeiite and mid–oceanic ridge basalt.

5–6 Chemical Analysis of Sea Floor Sediments

The chemical analyses of seventeen elements, relating to the hydrothermal activities and mineralization, were conducted for the muddy sediments collected by LC, FPG and CB. A total of 141 samples, consisting of 130 samples collected by LC at 19 sites, 2 samples collected by FPG at 2 sites and 9 samples collected by CB at nine sites, were chosen for the chemical analyses. The results are shown in Table 5–6–1 (1)–(4).

Table 5-6-1(1) Results of chemical analysis of sea floor sediments

Sample No.	Sampling depth	Au	Ag	As	Sb	Cs	Ca	Ba	S	Cu	Pb	Zn	Mn	Fe	Co	Ni	Cr	Cd
	cm	ppb	ppb	ppm	ppm	ppm	ppm	ppm	ppm	ppm	ppm	ppm	ppm	ppm	ppm	ppm	ppm	ppm
95SLC03 M1	5-10	<2	16.20	6.3	0.3	0.4	61743	223	800	47	5	26	2650	69384	24	14	13	<1
95SLC03 M2	45-50	<2	8.83	1.3	0.1	0.3	42409	181	500	16	1	10	107	54976	16	2	9	<1
95SLC03 M3	70-75	<2	12.60	15.1	0.4	0.4	88557	263	1090	133	16	99	11400	70014	27	62	20	<1
95SLC03 M4	100-105	<2	12.50	6.7	0.3	0.4	83759	172	1160	66	8	42	5530	71203	27	39	23	<1
95SLC04 M1	5-10	5	17.90	5.7	0.2	0.4	57933	215	870	42	4	22	2350	69454	24	13	11	<1
95SLC04 M2	35-40	8	14.30	16.5	0.4	0.3	90815	306	1140	128	19	101	11900	60571	24	58	15	<1
95SLC04 M3	55-60	10	9.75	2.2	0.1	0.6	33870	272	710	21	2	14	967	31754	9	7	10	<1
95SLC04 M4	90-95	2	13.00	5.7	0.3	0.4	87710	213	870	57	7	33	4830	71412	53	28	17	<1
95SLC05 M1	5-10	<2	15.80	6.5	0.1	0.6	55039	195	950	86	4	44	3550	75189	27	16	28	<1
95SLC05 M2	20-25	<2	38.50	3.5	0.1	0.3	57439	161	1540	83	2	32	563	74980	27	7	25	<1
95SLC05 M3	35-40	<2	10.70	7.1	0.2	0.4	39022	227	860	34	2	18	2260	56375	17	6	8	<1
95SLC05 M4	65-70	<2	21.00	1.5	0.1	0.3	54193	173	950	14	<1	7	138	71063	25	2	32	<1
95SLC05 M5	85-90	<2	19.00	2.5	0.1	0.3	55604	170	1140	26	1	10	397	75399	25	4	10	<1
95SLC07 M1	0-5	<2	16.60	7.4	0.2	0.6	64072	213	880	87	5	44	3270	75609	24	17	23	<1
95SLC07 M2	35-40	<2	12.50	5.3	0.1	0.3	42903	210	800	30	2	17	394	58403	15	4	8	<1
95SLC07 M3	70-75	11	19.80	2.1	0.1	0.3	58638	172	1060	25	1	8	260	77568	26	3	10	<1
95SLC07 M4	90-95	<2	16.90	1.0	0.1	0.3	60402	163	940	17	1	7	203	77498	13	3	11	<1
95SLC08 M1	0-5	<2	18.40	9.3	0.2	0.7	67247	231	1000	98	8	53	4190	74000	24	24	18	<1
95SLC08 M2	15-20	16	16.60	6.4	0.2	0.4	44384	239	680	33	3	19	1640	54626	14	8	8	<1
95SLC08 M3	55-60	<2	12.80	0.3	0.1	0.3	63648	156	720	8	<1	3	41	75819	27	3	19	<1
95SLC08 M4	65-70	<2	19.40	10.0	0.2	0.3	77620	633	980	85	8	41	6140	68964	23	23	8	<1
95SLC08 M5	80-85	<2	17.70	16.8	0.3	0.4	74162	314	1010	88	11	59	11000	56375	19	25	20	<1
95SLC09 M1	5-10	<2	20.20	7.3	0.2	0.3	54545	253	880	51	5	28	2810	56025	16	9	8	<1
95SLC09 M2	50-55	5	16.80	6.8	0.2	0.4	66188	228	930	58	5	29	3250	72182	24	12	13	<1
95SLC10 M1	5-10	<2	19.80	8.2	0.2	0.4	64001	281	860	61	9	40	4070	66936	23	14	10	<1
95SLC10 M2	25-30	13	16.30	7.6	0.2	0.4	62025	259	750	100	13	75	3320	69384	23	12	9	<1
95SLC10 M3	35-40	<2	21.30	8.8	0.2	0.4	69011	267	850	103	14	97	4280	71902	24	15	12	<1
95SLC10 M4	55-60	11	15.10	4.2	0.2	0.4	52005	223	780	32	3	25	1780	60082	17	7	13	<1
95SLC13 M1	5-10	<2	24.80	7.8	0.2	0.4	62307	261	860	53	5	27	4610	69174	21	16	11	<1
95SLC13 M2	25-30	<2	16.60	4.2	0.2	0.3	59767	201	810	39	3	17	1580	74140	24	7	8	<1
95SLC13 M3	65-70	4	12.80	<0.2	0.1	0.3	63930	158	860	8	<1	3	102	74910	24	2	12	<1
95SLC13 M4	80-85	<2	12.30	6.6	0.2	0.4	63013	232	850	60	4	26	4010	73091	26	13	12	<1
95SLC13 M5	105-110	8	15.50	7.6	0.2	0.3	65977	238	980	60	5	28	3910	75119	25	13	11	<1
95SLC14 M1	5-10	<2	21.30	8.0	0.2	0.4	66118	268	990	54	6	28	4030	64978	22	14	11	<1
95SLC14 M2	25-30	<2	18.90	8.1	0.2	0.4	68588	265	750	66	6	33	4140	68685	23	15	10	<1
95SLC14 M3	35-40	<2	15.90	8.0	0.2	0.4	69858	247	900	66	6	34	4350	71972	25	17	9	1
95SLC14 M4	50-55	<2	19.70	7.8	0.2	0.3	62237	248	840	55	5	28	3340	62110	18	11	11	<1

Table 5-6-1 (2) Results of chemical analysis of sea floor sediments

Sample No.	Sampling depth	Au	Ag	As	Sb	Cs	Ca	Ba	S	Cu	Pb	Zn	Mn	Fe	Co	Ni	Cr	Cd
	cm	ppb	ppb	ppm	ppm	ppm	ppm	ppm	ppm	ppm	ppm	ppm	ppm	ppm	ppm	ppm	ppm	ppm
95SLC14 M5	80-85	<2	14.30	3.4	0.1	0.3	41562	202	680	19	1	13	765	52807	12	2	6	<1
95SLC15 M1	5-10	19	23.50	9.9	0.2	0.6	68305	246	1110	107	6	54	4350	74000	26	15	20	<1
95SLC15 M2	15-20	11	36.30	4.3	0.1	0.4	63013	175	1330	72	2	27	734	74140	24	6	23	<1
95SLC17 M1	5-10	11	25.50	11.7	0.2	0.6	79525	254	1160	79	7	38	4050	69594	22	15	18	<1
95SLC17 M2	30-35	<2	20.10	7.5	0.2	0.3	71057	228	1020	56	4	26	3070	72532	25	12	12	<1
95SLC17 M3	50-55	<2	15.70	5.5	0.1	0.4	70140	201	820	45	3	21	2060	76518	26	9	13	<1
95SLC17 M4	80-85	7	22.10	5.9	0.2	0.3	70493	205	900	54	3	22	1840	77008	26	7	12	<1
95SLC19 M1	5-10	<2	13.30	6.0	0.2	0.5	54828	200	940	102	3	47	2950	77847	28	9	23	<1
95SLC19 M2	30-35	14	37.60	5.6	0.1	0.3	56662	186	1760	93	3	41	1020	76378	25	7	19	<1
95SLC19 M3	45-50	8	29.50	4.5	0.1	0.3	56804	178	1630	80	2	33	966	73581	26	7	20	<1
95SLC19 M4	65-70	9	27.00	2.9	0.1	0.4	60685	675	1630	59	1	21	607	74140	25	4	20	<1
95SLC21 M1	5-10	<2	13.00	3.8	0.2	0.4	59203	168	720	62	1	27	1590	73301	25	6	25	<1
95SLC21 M2	25-30	<2	10.40	4.1	0.1	0.4	61037	193	890	36	2	15	902	73161	25	5	10	<1
95SLC21 M3	45-50	<2	16.10	7.4	0.2	0.4	69434	213	880	65	5	30	2890	73860	25	13	24	<1
95SLC21 M4	70-75	<2	17.40	1.8	0.1	0.4	63013	168	710	20	1	10	313	77707	26	3	13	<1
95SLC21 M5	90-95	7	14.70	4.0	0.1	0.3	61955	188	830	46	2	17	1460	77637	28	6	11	<1
95SLC26 M1	5-10	<2	18.50	13.0	0.2	0.4	86158	306	1120	84	8	43	5590	72112	26	19	14	<1
95SLC26 M2	30-35	8	16.00	5.6	0.2	0.3	65906	206	760	56	3	23	2270	77008	27	7	13	<1
95SLC26 M3	45-50	<2	12.60	3.0	0.2	0.3	60685	177	720	35	1	14	1770	76588	25	5	11	<1
95SLC26 M4	65-70	<2	17.00	2.7	0.1	0.3	66471	222	800	69	4	25	1590	73721	24	6	13	<1
95SLC26 M5	90-95	<2	11.10	5.1	0.1	0.4	59626	208	970	54	2	20	999	72252	23	7	14	<1
95SLC26 M6	110-115	9	14.00	11.4	0.2	0.5	73950	241	930	101	8	58	4030	73231	24	19	16	<1
95SLC26 M7	125-130	4	18.20	18.3	0.3	0.3	92367	306	1090	128	12	71	8810	66866	23	27	20	1
95SLC26 M8	155-160	10	13.70	3.2	0.2	0.4	44455	237	890	32	1	14	2730	47212	14	8	12	<1
95SLC26 M9	170-175	4	13.80	3.0	0.1	0.5	39727	272	860	23	1	14	613	41337	9	4	9	<1
95SLC26 M10	190-195	<2	15.80	13.6	0.2	0.5	85170	373	870	70	8	35	4900	50499	18	15	24	<1
95SLC27 M1	5-10	10	15.70	5.7	0.1	0.5	65130	192	920	91	3	38	1640	72462	23	9	19	<1
95SLC27 M2	20-25	11	15.00	4.9	0.1	0.4	69787	210	860	63	2	22	1290	73021	25	6	19	<1
95SLC27 M3	35-40	<2	13.20	4.9	0.1	0.4	59767	201	1280	48	2	21	671	72182	21	5	13	<1
95SLC27 M4	70-75	<2	13.00	4.7	0.2	0.4	67529	195	850	54	2	24	1220	69524	24	6	14	<1
95SLC27 M5	95-100	<2	10.40	2.7	0.1	0.4	55039	190	760	52	2	23	512	65747	23	5	21	<1
95SLC27 M6	125-130	<2	80.70	1.2	0.1	0.3	63084	121	890	76	<1	13	200	78617	32	4	35	<1
95SLC27 M7	155-160	<2	17.00	3.8	0.2	0.3	176691	127	940	34	2	18	1170	34132	11	4	19	<1
95SLC27 M8	170-175	<2	13.50	3.5	0.2	0.3	141903	149	1080	24	2	17	774	42945	15	5	20	1
95SLC27 M9	185-190	<2	14.40	5.1	0.2	0.5	67811	185	830	51	2	23	608	72042	26	6	24	<1
95SLC27 M10	205-210	<2	28.20	4.9	0.1	0.4	71269	223	770	64	3	23	539	60361	22	8	55	<1

Table 5-6-1(3) Results of chemical analysis of sea floor sediments

Sample No.	Sampling depth	Au	Ag	As	Sb	Cs	Ca	Ba	S	Cu	Pb	Zn	Mn	Fe	Co	Ni	Cr	Cd
	cm	ppb	ppb	ppm	ppm	ppm	ppm	ppm	ppm	ppm	ppm	ppm	ppm	ppm	ppm	ppm	ppm	ppm
95SLC28 M1	5-10	<2	15.80	6.1	0.2	0.6	60614	200	950	84	3	36	2130	75889	27	11	21	<1
95SLC28 M2	15-20	<2	21.10	15.0	0.3	0.3	88769	309	1230	87	8	43	6410	70713	27	21	19	<1
95SLC28 M3	45-50	<2	12.50	5.4	0.2	0.3	63860	203	960	56	3	23	3000	77078	27	9	15	<1
95SLC28 M4	70-75	<2	29.60	3.4	0.1	0.3	61108	173	1210	38	2	16	730	75050	25	5	12	<1
95SLC28 M5	85-90	17	24.60	2.3	0.1	0.3	61390	166	950	28	1	11	669	75609	29	4	15	<1
95SLC28 M6	105-110	18	17.30	6.5	0.2	0.3	66188	224	900	71	3	23	2240	75119	26	10	16	<1
95SLC28 M7	135-140	<2	25.50	2.8	0.1	0.4	59273	176	1170	37	1	12	700	75119	26	4	13	<1
95SLC28 M8	160-165	<2	19.60	1.6	0.1	0.3	59697	175	880	25	1	8	563	76099	26	4	17	<1
95SLC28 M9	180-185	12	10.80	5.8	0.1	0.3	58991	220	1050	57	2	20	1450	72741	25	7	16	<1
95SLC28 M10	205-210	<2	17.20	9.8	0.2	0.3	67600	245	1010	69	6	36	2610	67286	24	12	20	<1
95SLC28 M11	230-235	<2	18.60	13.0	0.3	0.4	82489	264	1040	108	8	50	5370	72602	25	21	18	<1
95SLC28 M12	250-255	<2	13.60	6.6	0.2	0.4	49183	254	1060	43	3	23	3190	47282	14	10	15	<1
95SLC29 M1	0-5	<2	17.60	8.1	0.2	0.7	70563	244	1150	82	4	43	3410	71902	27	15	25	<1
95SLC29 M2	5-15	<2	21.80	16.5	0.3	0.3	97871	328	1260	96	9	47	7160	68405	26	25	17	<1
95SLC29 M3	15-25	<2	16.30	9.2	0.2	0.3	79102	256	1070	68	5	32	4290	73581	27	16	14	<1
95SLC29 M4	25-35	18	15.70	9.3	0.2	0.3	78678	252	950	71	6	32	3930	73161	26	15	17	<1
95SLC29 M5	35-45	17	16.00	13.9	0.2	0.3	83194	278	1110	93	9	46	5650	69034	24	20	19	<1
95SLC29 M6	45-55	20	13.20	9.9	0.2	0.4	72116	221	980	83	6	45	3930	74280	27	14	21	<1
95SLC29 M7	55-65	12	13.20	22.1	0.3	0.3	111278	336	1180	130	14	75	11200	62520	23	37	22	1
95SLC29 M8	65-75	<2	16.10	10.4	0.2	0.4	68094	300	990	64	7	36	5670	52248	17	18	16	<1
95SLC29 M9	75-85	<2	13.90	9.4	0.2	0.3	83053	270	1020	61	6	33	5400	58753	21	17	21	<1
95SLC29 M10	85-95	<2	15.60	10.4	0.2	0.4	70916	340	1010	58	7	29	5320	42736	15	16	18	<1
95SLC29 M11	95-105	<2	12.20	1.3	0.1	0.5	34717	289	750	16	1	7	548	34272	9	5	11	<1
95SLC29 M12	105-115	17	16.20	12.6	0.3	0.5	95896	335	1140	76	8	38	5350	69034	28	16	21	<1
95SLC29 M13	115-125	<2	9.45	5.0	0.1	0.6	70069	223	790	55	3	25	2150	72811	28	8	26	<1
95SLC29 M14	125-135	<2	11.60	5.9	0.2	0.4	63578	212	990	53	3	28	2660	69594	24	10	20	<1
95SLC29 M15	135-145	<2	14.10	6.5	0.2	0.5	66400	273	1030	45	4	27	2490	61061	20	10	19	<1
95SLC29 M16	145-155	7	13.30	5.7	0.1	0.4	69152	249	840	49	3	23	2020	63719	23	8	26	<1
95SLC29 M17	155-165	<2	16.90	3.4	0.1	0.4	68023	176	650	52	2	23	1180	71762	30	6	35	<1
95SLC29 M18	165-175	13	16.50	7.1	0.2	0.4	80372	243	880	62	4	27	3260	67845	24	12	21	<1
95SLC29 M19	175-185	<2	12.70	15.4	0.3	0.3	107680	343	1020	85	10	41	6340	64138	26	17	34	<1
95SLC29 M20	185-195	<2	15.80	6.5	0.2	0.7	69787	219	870	74	4	31	3030	71273	27	12	22	<1
95SLC29 M21	195-205	<2	15.40	17.4	0.3	0.4	112619	343	1250	100	13	51	7760	60851	23	23	24	<1
95SLC29 M22	205-215	9	12.60	10.7	0.2	0.5	92650	269	990	77	7	37	5610	65887	25	18	26	<1
95SLC29 M23	215-225	13	12.00	11.4	0.2	0.4	84535	315	1040	63	8	37	5930	57074	18	17	15	<1
95SLC29 M24	225-235	<2	9.32	2.3	0.1	0.5	46078	215	760	24	1	15	705	53996	13	5	9	<1
95SLC29 M25	235-245	<2	11.20	5.8	0.1	0.4	76702	246	870	55	4	25	2100	62600	23	6	28	<1

Table 5-6-1(4) Results of chemical analysis of sea floor sediments

Sample No.	Sampling depth	Au	Ag	As	Sb	Cs	Ca	Ba	S	Cu	Pb	Zn	Mn	Fe	Co	Ni	Cr	Cd
	cm	ppb	ppb	ppm	ppm	ppm	ppm	ppm	ppm	ppm	ppm	ppm	ppm	ppm	ppm	ppm	ppm	ppm
95SLC29 M26	245-255	8	13.60	11.1	0.3	0.4	102176	282	1110	76	9	37	5610	63789	26	18	31	<1
95SLC29 M27	255-265	<2	10.40	11.0	0.2	19.4	88063	287	950	72	9	37	5980	63089	24	18	21	<1
95SLC29 M28	265-275	6	11.30	4.0	0.1	0.8	50029	249	780	36	3	22	1730	58193	17	8	6	<1
95SLC29 M29	275-285	21	12.20	2.7	0.1	0.4	49465	217	860	29	2	17	374	58403	16	2	9	<1
95SLC30 M1	5-10	<2	19.00	7.4	0.2	0.3	55604	181	970	79	4	35	1870	63229	20	10	15	<1
95SLC30 M2	25-30	15	15.20	8.8	0.2	0.4	75503	243	1090	66	5	30	3970	73791	27	14	11	<1
95SLC30 M3	50-55	14	14.10	5.0	0.2	0.4	61390	200	850	51	3	20	2520	74070	25	9	14	<1
95SLC30 M4	65-70	<2	19.00	5.1	0.2	0.3	56521	196	990	50	2	18	2280	70993	24	8	14	<1
95SLC30 M5	80-85	10	19.10	7.5	0.1	0.4	61178	205	830	75	4	36	2530	74840	27	10	18	<1
95SLC30 M6	105-110	16	26.80	14.3	0.2	0.4	83829	265	1060	99	9	50	5010	66237	24	19	20	<1
95SLC30 M7	145-150	<2	18.90	1.6	0.1	0.5	39092	259	910	17	1	11	380	41127	9	3	12	<1
95SLC30 M8	155-160	<2	20.00	12.4	0.2	0.4	92015	310	960	68	7	33	3870	60431	23	13	22	1
95SLC31 M1	5-10	9	17.60	7.6	0.2	0.5	64142	227	1000	83	4	40	2540	74420	27	12	18	<1
95SLC31 M2	25-30	7	17.10	8.1	0.2	0.4	75362	244	1020	59	5	28	3840	74420	26	15	13	<1
95SLC31 M3	45-50	<2	11.80	5.1	0.1	0.3	64424	210	940	52	3	21	2080	74910	24	8	15	<1
95SLC31 M4	70-75	15	16.60	8.0	0.2	0.5	65836	212	850	72	4	34	2530	73161	25	11	18	<1
95SLC31 M5	95-100	12	22.10	17.3	0.3	0.3	98506	294	1160	100	11	54	8220	65327	25	25	24	<1
95SLC31 M6	115-120	<2	15.70	6.0	0.2	0.4	54475	242	970	46	3	22	2520	52947	16	11	15	<1
95SLC31 M7	135-140	<2	18.40	2.8	0.1	0.5	39374	263	770	20	1	13	645	41267	9	4	7	<1
95SLC31 M8	145-150	10	27.90	11.1	0.2	0.4	99353	284	980	69	7	33	3920	62530	24	13	24	1
95SFPG01		9	14.90	8.9	0.2	0.2	190803	234	1100	46	8	33	3180	40218	19	21	80	1
95SFPG02		<2	17.90	5.3	0.2	0.3	48406	287	650	35	5	22	1270	49100	13	6	8	<1
95SCB01		14	36.20	14.6	0.4	0.4	91732	329	1340	91	14	50	8000	63928	22	27	18	<1
95SCB02		<2	20.40	13.6	0.2	0.4	81218	279	1350	90	13	51	6820	57704	21	24	13	<1
95SCB03		14	25.30	10.7	0.2	0.7	81007	315	1290	109	16	86	5540	66586	23	19	19	<1
95SCB05		10	21.00	6.3	0.2	0.4	68729	193	890	79	7	51	2900	74070	26	17	51	<1
95SCB06		11	21.40	5.9	0.2	0.3	75432	156	800	52	10	34	2610	76728	32	20	45	<1
95SCB07		18	37.20	13.0	0.3	0.4	84747	254	1380	108	11	74	5570	70993	28	27	61	<1
95SCB09		<2	24.50	12.1	0.2	0.4	69293	249	1340	93	7	51	4460	59032	19	17	18	<1
95SCB10		8	24.70	11.3	0.2	0.5	70140	256	1310	91	6	49	4410	64488	21	16	19	<1
95SCB11		<2	20.00	7.6	0.2	0.4	88204	260	1270	73	5	36	3110	67006	25	14	22	<1

(1) Analytical Method

The analytical methods, together with analyzed elements, are shown below. The numbers in the parenthesis following the each element denote the detection limit. After drying until reaching to the constant weight, sample preparation was conducted.

- ICP: Au(2ppb), Au(0.02ppm), As(0.2ppm), Sb(0.2ppm), Cs(0.1ppm), Ca, Ba, Cu, Pb, Zn, Mn, Fe, Co, Ni, Cr, Cd (from Ca to Cd: 0.1ppm)

- XRF: S(50ppm)

(2) Statistical Analysis

The statistical analysis of the analytical results consists of the calculation of basic statistics and the multivariate analysis. The values less than detection limit are replaced with the half value of the detection limit. Cd is excluded for this analysis, since almost samples show the value below than the detection limit. Because geochemical data generally shows a normal distribution in logarithm, the analytical values are converted to logarithm for the following analysis.

1) Basic Statistics

The basic statistics are given in Table 5−6−2. The reason for high Ca is that the sea floor sediments include calcium carbonate of organic origin such as microfossils. Similarly, the sea floor sediments are rich in Mn and Fe because they include considerable amount of Mn−Fe oxides.

The average values of the basalt (Table 5−5−3) are also given in Table 5−6−2. A comparison of these average values shows that eight elements of Au, Ag, As, Sb, Cs, Ba, Pb and Mn are higher in the sea floor sediments than in the basalt. Among these, As and Ba show large differences. While, S and Cr are less in the sea floor sediments than in basalt. The averages of the base metal elements (such as Cu, Pb, Zn and Fe), which are related to the minerals occurring in the submarine hydrothermal deposits, are not clearly high to indicate the hydrothermal activities.

2) Multivariate Analysis.

The factor analysis, one of the multivariate analysis, was conducted for 16 elements (Cd is excluded.) of 141 samples. The communality is estimated from the multiple correlation coefficients. After the varimax rotation, factor loadings and factor scores are calculated. The correlation coefficients and factor loadings are, respectively, shown in Tables 5−6−3 and 5−6−4.

As given in Table 5−6−4, following elements of two groups show mutually high positive correlation coefficients in each group.

Table 5-6-2 Basic statistics

Component name	Unit	Number of sample	Maximum	Minimum	Mean (M)	Std. dev. (SD)	M−2×SD	M−SD	M+SD	M+2×SD	Mean of rock samples
Au	ppb	141	21	1	2.6	0.51	0.2	0.8	8.3	26.7	<1
Ag	ppb	141	80.7	8.83	16.894	0.141	8.83	12.214	23.368	32.323	15.74
As	ppm	141	22.1	0.1	5.89	0.33	1.29	2.75	12.6	26.96	0.44
Sb	ppm	141	0.4	0.1	0.17	0.171	0.08	0.11	0.25	0.37	0.1
Cs	ppm	141	19.4	0.2	0.4	0.176	0.18	0.26	0.59	0.89	0.1
Ca	ppm	141	190803	33870	67528.8	0.116	39565.6	51689.7	88221.4	115255	79031
Ba	ppm	141	675	121	232	0.107	141.5	181.2	297.1	380.4	32
S	ppm	141	1760	500	956.2	0.085	645.3	785.5	1163.9	1416.7	6454
Cu	ppm	141	133	8	55.1	0.236	18.6	32	94.8	163.1	82
Pb	ppm	141	19	0.5	3.67	0.362	0.69	1.59	8.44	19.43	1
Zn	ppm	141	101	3	27	0.263	8	14.7	49.5	90.7	66
Mn	ppm	141	11900	41	2100.3	0.455	258.5	736.8	5987.3	17067.9	1366
Fe	ppm	141	78617	31754	65676.3	0.079	45731.3	54803.9	78705.9	94320.3	77651
Co	ppm	141	53	9	22.2	0.12	12.7	16.8	29.3	38.6	42
Ni	ppm	141	62	2	10	0.302	2.5	5	20	40	86
Cr	ppm	141	80	6	16.3	0.194	6.7	10.4	25.5	39.9	287

Standard deviation (std. dev.) is shown in logarithmic scale.

Table 5-6-3 Correlation coefficient

	Au	Ag	As	Sb	Cs	Ca	Ba	S	Cu	Pb	Zn	Mn	Fe	Co	Ni	Cr
Au	—	141	141	141	141	141	141	141	141	141	141	141	141	141	141	141
Ag	.149	—	141	141	141	141	141	141	141	141	141	141	141	141	141	141
As	.162	.099	—	141	141	141	141	141	141	141	141	141	141	141	141	141
Sb	.067	.042	.714	—	141	141	141	141	141	141	141	141	141	141	141	141
Cs	-.032	-.177	.133	.029	—	141	141	141	141	141	141	141	141	141	141	141
Ca	.120	.126	.512	.554	-.047	—	141	141	141	141	141	141	141	141	141	141
Ba	.109	-.022	.577	.435	.166	.209	—	141	141	141	141	141	141	141	141	141
S	.192	.477	.400	.263	-.036	.413	.265	—	141	141	141	141	141	141	141	141
Cu	.199	.293	.842	.586	.133	.500	.399	.492	—	141	141	141	141	141	141	141
Pb	.183	.080	.880	.752	.142	.593	.578	.338	.791	—	141	141	141	141	141	141
Zn	.197	.174	.889	.663	.170	.489	.484	.420	.931	.895	—	141	141	141	141	141
Mn	.152	.004	.911	.786	.166	.519	.590	.331	.796	.896	.856	—	141	141	141	141
Fe	.100	.232	.030	.002	-.063	.094	-.245	.166	.329	.043	.133	.029	—	141	141	141
Co	.127	.219	.214	.200	-.040	.407	-.138	.254	.486	.257	.306	.238	.858	—	141	141
Ni	.145	.098	.841	.792	.149	.573	.529	.395	.800	.916	.859	.917	.092	.335	—	141
Cr	.120	.246	.239	.199	.058	.557	-.044	.322	.414	.260	.342	.196	.147	.423	.336	—

Note : Correlation coefficients are written in left-bottom side.
Numbers of data are written in left-bottom side.

Table 5-6-4 Results of factor analysis

Component name	Factor loadings					Communalities
	First factor	Second factor	Third factor	Fourth factor	Fifth factor	
Au	0.122	0.064	0.222	-0.040	-0.016	0.070
Ag	-0.036	0.108	0.723	-0.071	0.160	0.567
As	0.893	0.030	0.222	-0.092	-0.167	0.885
Sb	0.812	0.030	0.006	-0.171	0.159	0.714
Cs	0.131	-0.041	-0.121	-0.014	-0.378	0.176
Ca	0.511	0.110	0.120	-0.629	0.249	0.745
Ba	0.614	-0.254	0.110	0.112	-0.104	0.477
S	0.290	0.054	0.619	-0.193	0.097	0.517
Cu	0.724	0.309	0.436	-0.187	-0.307	0.939
Pb	0.923	0.058	0.131	-0.162	-0.098	0.909
Zn	0.828	0.131	0.313	-0.155	-0.320	0.928
Mn	0.958	0.063	0.067	-0.080	-0.116	0.946
Fe	-0.035	0.958	0.182	0.036	0.029	0.955
Co	0.155	0.879	0.143	-0.312	0.049	0.917
Ni	0.902	0.117	0.132	-0.219	-0.086	0.900
Cr	0.088	0.147	0.256	-0.803	-0.152	0.763

- As, Sb, Cu, Pb, Zn, Mn, Ni
- Fe, Co

Except for these relations, neither positive nor negative high correlation coefficients exist. The results of factor analysis, also, show the large contribution of these two groups of elements.

In the factor analysis, the number of factors is decided as 5 from the eigenvalue and cumulative contribution. The results of the factor analysis is given below on each factor.

① Factor 1 (F1)

The factor loading of the each element suggests that As, Sb, Ba, Cu, Pb, Zn, Mn and Ni contribute to F1. This factor seems to be related to hydrothermal activities, but hydrothermal activities are not observed in this survey. Since manganese oxides are attached on the surface of older rock, F1 can be related to the precipitation of manganese on the sea floor. The elements given above are enriched together with manganese oxides in the sea floor sediments.

The samples with high F1 factor score have higher concentration of the above elements.

② Factor 2 (F2)

Fe and Co are related to F2. This factor is related to the enrichment of Fe and Co, but the cause of this enrichment is unknown. The form of Fe and Co in the sea water (for example, a complex ion is formed or not, the kind of complex ion) and the precipitating way of these (direct precipitation from the sea water, or precipitation from the pore water in the sediments) is different from that of other elements, so that Fe and Co seperately contribute to F2.

The samples with high F2 factor score correspond to the samples of high Fe.

③ Factor 3 (F3)

Ag and S are related to F3. This seems to be related to hydrothermal activities, but no clear evidence is found. The samples with high F3 factor score correspond to the samples of high Ag and S.

④ Factor 4 (F4)

Ca and Cr are related to F4. Calcareous microfossils and the concentration of mafic minerals of volcanic rocks are considered to be the factors controlling F4. The samples with high F4 factor score correspond to the samples with high Ca and Cr.

⑤ Factor 5 (F5)

Cs, Cu and Pb show a slightly higher factor loading, but since there are no elements clearly showing high factor loadings of F5, the interpretation of F5 is difficult.

(3) Consideration of the Analytical Results

From the consideration of the relations among characters of muddy sediments, sampling depth and analytical results, the following characteristic tendencies are obtained. In order to study the change of analytical value against the sampling depth in each LC, bar graphs of analytical value for Mn, Cu and Ag, which represent each factor (F1 to F3), are made (Fig. 5–6–1 (1) to (3)). In this figure, the letters after the LC No. (M1 to M29) mean the difference of sampling depth. The actual sampling depths are shown in APPENDIX Table 4 (1) – (3).

1) Relation between the nature and the analytical value of LC samples.

- The black to dark gray volcanic ash and volcanic sand have clearly lower Mn and slightly lower Cu, Pb and Zn compared with the normal muddy sediments.
- Olive mud is lower in Mn compared with brown mud.

2) Relation between the sampling depth and the analytical value of LC samples (See Fig. 5–6–1)

- There is no clear relation between the sampling depth and the analytical value.
- Depending on the LC site, some elements decrease the values as the sampling depth increases. The example is Mn of 95SLC17, samples of which are brown mud.

3) Relation between the location and the analytical value of LC samples

- There is no clear relation between the location of LC (relative location on south–north direction, distance from the spreading center and topography) and the analytical values.

4) Conclusions

- The analytical values of As, Sb, Ba, Cu, Pb, Zn, Mn and Ni (contributing to F1 in factor analysis) are low in the volcanic sediments (volcanic ash and sand), and high in the ordinary sea floor sediments (muddy sediments).
- The vertical variations of chemical composition seem to be controlled by the environments of sedimentation rather than by the depth of sediments.
- On the basis of the vertical variations of chemical composition, there is no evidence of intensive regional hydrothermal activities at the certain time, because the geochemical anomalies occur very locally.

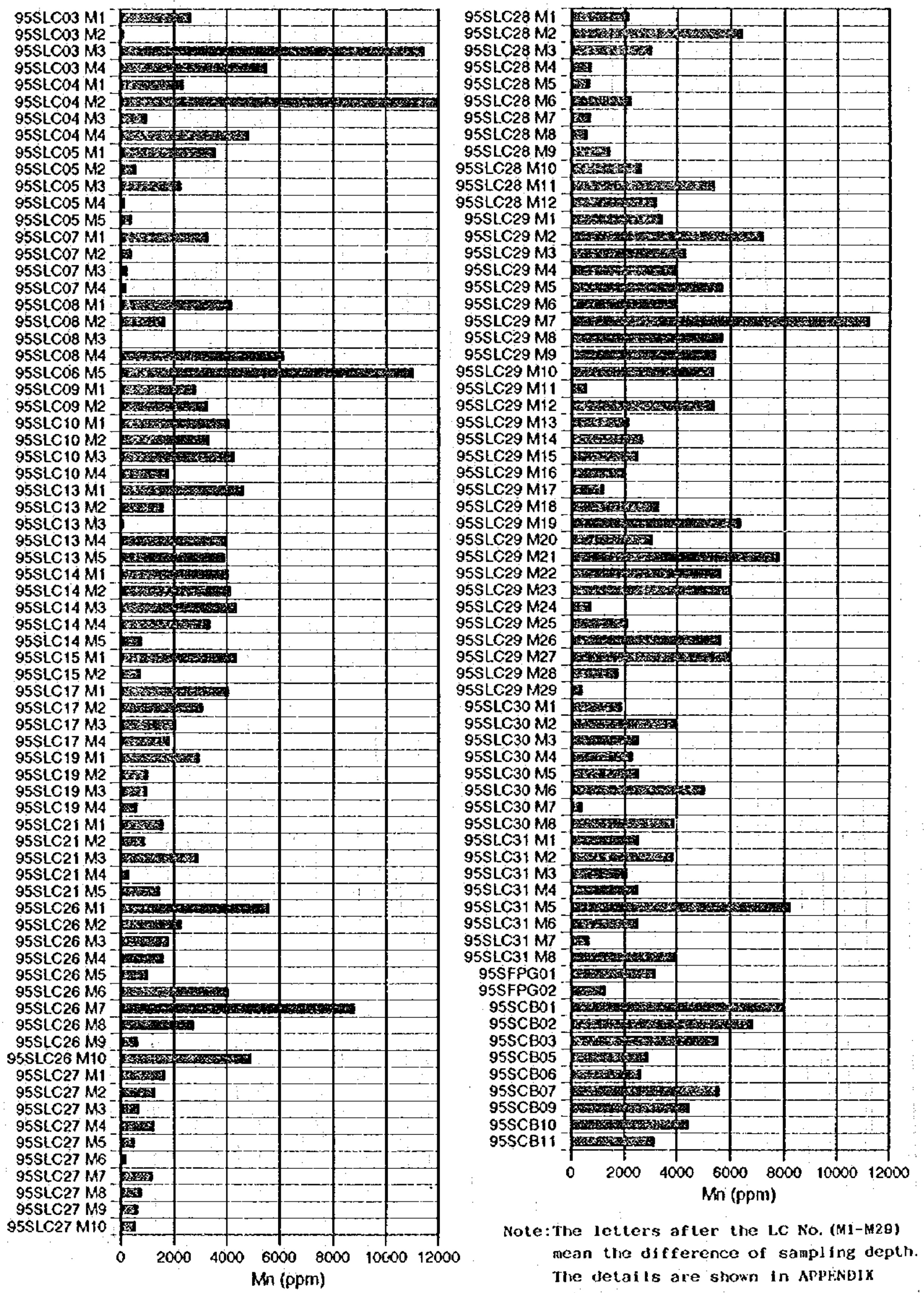

Note:The letters after the LC No. (M1-M29) mean the difference of sampling depth. The details are shown in APPENDIX Table 4 (1)-(3).

Fig. 5-6-1 (1) Bar graphs of chemical analysis data of sea floor sediments (Mn)

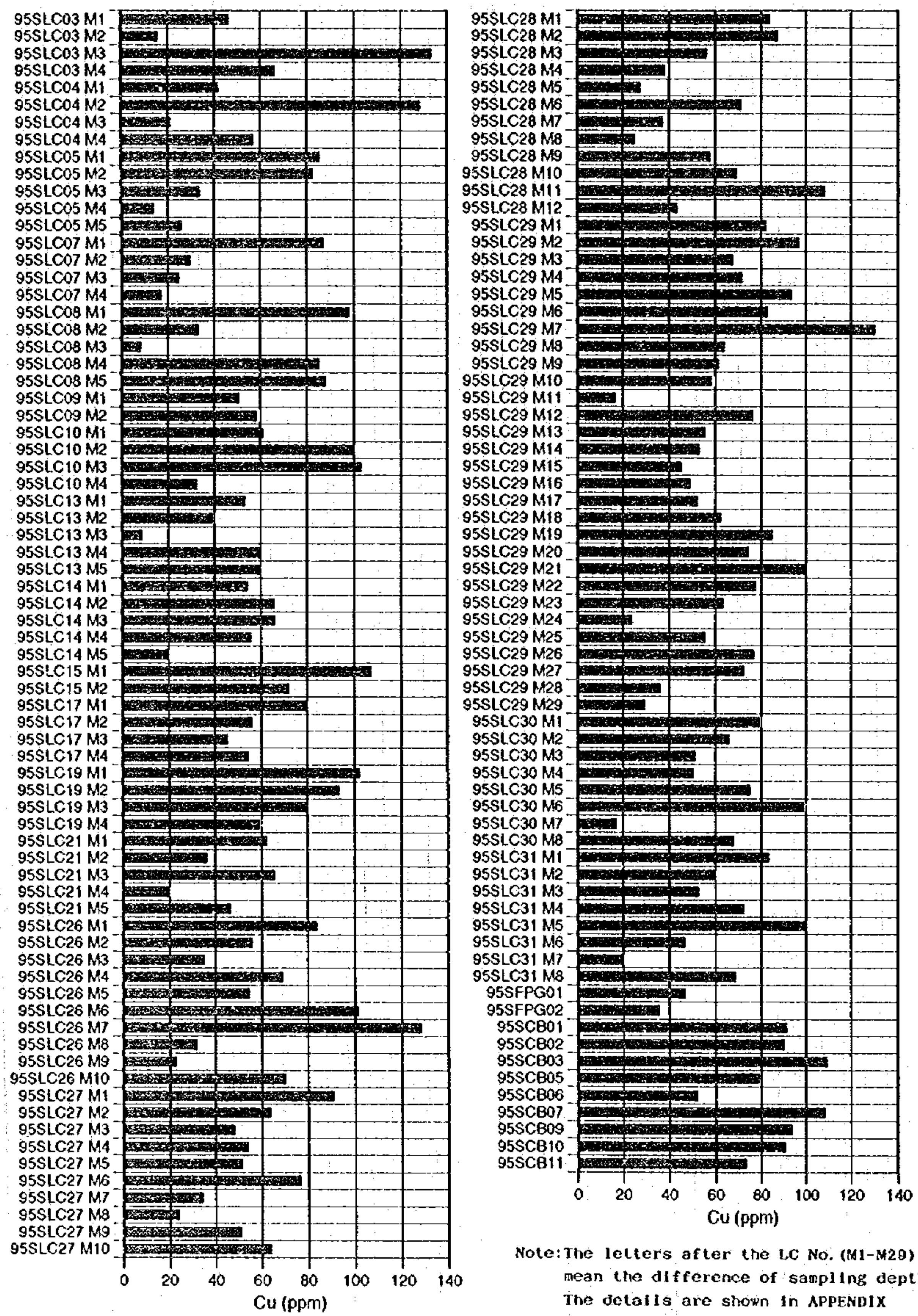

Note: The letters after the LC No. (M1-M29) mean the difference of sampling depth. The details are shown in APPENDIX Table 4 (1)-(3).

Fig. 5-6-1 (2) Bar graphs of chemical analysis data of sea floor sediments (Cu)

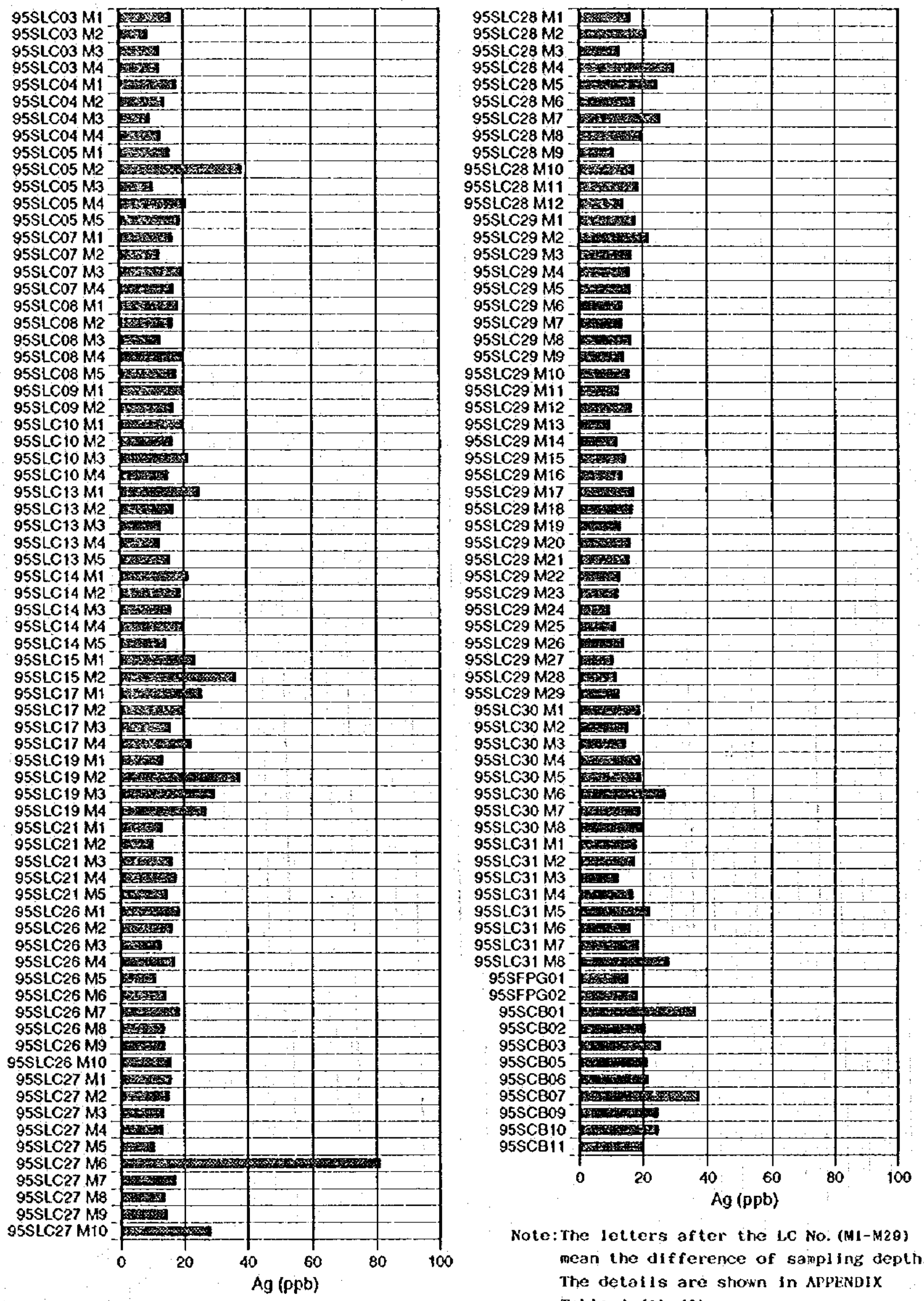

Note: The letters after the LC No. (M1-M29) mean the difference of sampling depth. The details are shown in APPENDIX Table 4 (1)-(3).

Fig. 5-6-1 (3) Bar graphs of chemical analysis data of sea floor sediments (Ag)

5-7 Microfossil in the Sea Floor Sediments

Among the sea floor sediments collected by LC and FPG, four samples were selected for the identification of foraminifera and radiolaria. The results are given in Table 5-7-1. The photographs of representative microfossils are shown in Fig. 5-7-1 (1), (2).

(1) Foraminifera

Abundant pieces of foraminifera are found in each of the four samples. The foraminiferas found in the four samples are predominantly planktonic foraminifera and benthonic foraminiferas are rarely found. The fossil zone is based on the classification of Blow (1969) and the geological period is based on Berggren et al. (1985) which is applicable for the lower latitude zone. The results are given below.

1) 95SLC15 (Depth: 10 to 15cm) (See Fig. 4-1-2 (2))

The planktonic foraminiferas are preserved well. The occurrence of *Globigerinella calida* suggests that the sample is classified to N23 zone (0 to 0.3 Ma). Because the sample contains abundant *Globigerinoides sacculifer*, it belongs to tropical or subtropical area.

2) 95SLC17 (Depth: 40 to 50 cm) (See Fig. 4-1-2 (2))

The planktonic foraminiferas are preserved well. The occurrence of *Globorotalia truncatulinoides* and the absence of *Globigerinella calida* suggest that the sample belongs to early to middle Pleistocene. Because the sample contains abundant *Globigerinoides sacculifer*, it belongs to tropical or subtropical area.

3) 95SFPG01 (See Fig. 4-1-2 (4))

The planktonic foraminiferas are preserved well. The occurrences of *Globorotalia truncatulinoides*, Globigerinella calida and dextral Pulleniatina (genus) suggest that the sample is classified to N23 zone (0 to 0.3 Ma). Because *Globigerrinoides ruber* is more abundant than *Globigerinoides sacculifer*, and *Globorotalia inflata*, which is common in the middle latitude area, occurs, the sample belongs to subtropical area.

4) 95SFPG02 (See Fig. 4-1-2 (4))

The planktonic foraminiferas are preserved very well. The occurrence of *Globigerinella calida* suggests that the sample is classified to N23 zone (0 to 0.3 Ma). Because the sample contains abundant

Table 5-7-1 Results of microscopic observation of microfossils

Foraminifera (Figures mean the number of fossils observed)

Species name	95SLC15 F	95SLC17F	95SFPG01F	95SFPG02F
Candeina nitida				2
Globigerinella aequilateralis	7	11	5	8
G. calida	1		2	3
Globigerinita glutinata	4			6
Globigerinoides conglobatus	10	13	15	13
G. ruber	26	29	40	24
G. sacculifer	27	39	27	51
Globorotalia crassaformis	4	5	7	12
G. inflata	1		10	
G. menardii			1	1
G. truncatulinoides		3	3	
G. tumida			1	1
Globorotaloides hexagonus			1	
Neogloboquadrina dutertrei			1	1
Orbulina universa	1	11	4	6
Pulleniatina obliquiloculata			2	1

Radiolaria (+ means the occurrence)

Species name	95SLC15 F	95SLC17F	95SFPG01F	95SFPG02F
Acrosphaera lappacea (Haeckel)	+			
Acrosphaera spinosa (Haeckel)	+	+	+	
Siphonosphaera sp.	+	+	+	
Axoprunum stauraxonium Haeckel	+	+	+	+
Cenosphaera spp.		+	+	+
Ellipsoxiphus atractus Haeckel	+	+	+	+
Heliosphaera inermis Haeckel		+		
Hexacontium anaximandri (Haeckel)		+		
Actinommidae genn. et spp. indet.	+			
Didymocyrtis tetrathalamus (Haeckel)		+		
Stylochlamydium asteriscus Haeckel	+			
Stylodictya multispina Haeckel		+	+	
Stylodictya camerina Campbell and Clark		+		
Dictyocoryne spp.	+			
Euchitonia furcata Ehrenberg	+	+		
Spongaster tetras tetras Ehrenberg	+			
other spongodiscids	+	+		
Hexapyle sp.		+		
Tetrapyle octacantha Muller		+		
Lithelius minor Jorgensen	+	+		
Spongurus cf. elliptica (Ehrenberg)		+		
Liriospyris costata (Haeckel) juvenile			+	
Carpocanistrum spp.		+	+	
Lamprocyclas maritalis Haeckel	+		+	
Theocorythium trachelium (Ehrenberg)		+	+	

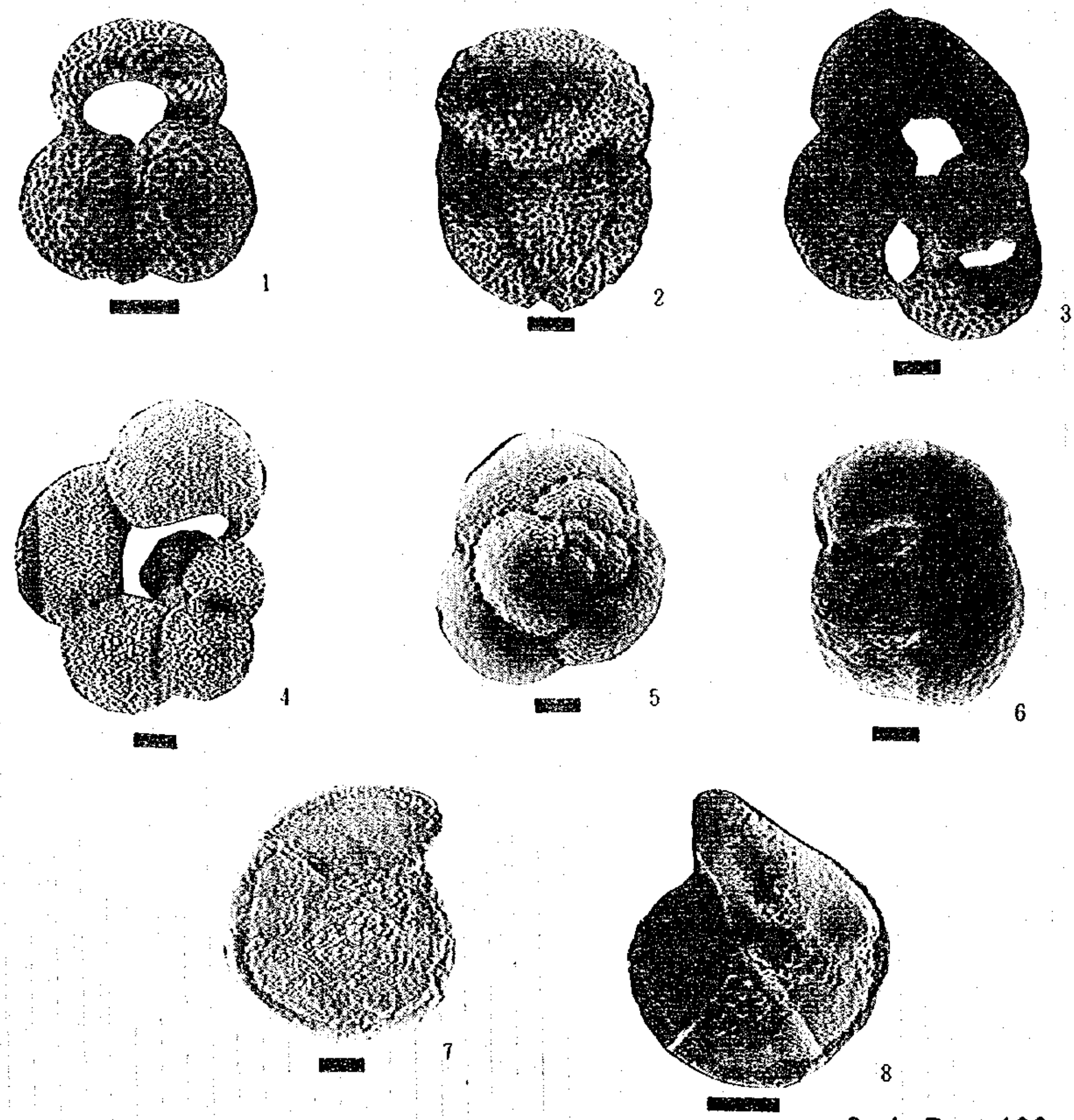

(Foraminifera)

Scale Bars: 100 μm

1. *Globigerinoides ruber* (d'Orbigny) 95SFPG01, umbilical view
2. *Globigerinoides conglobatus* (Brady) 95SLC17 40-50cm, side view
3. *Globigerinoides sacculifer* (Brady) 95SLC15, umbilical view
4. *Globigerinella aequilateralis* (Brady) 95SLC15, umbilical view
5. *Candeina nitida* d'Orbigny 95SFPG02, spiral view
6. *Globorotalia inflata* (d'Orbigny) 95SLC15, spiral view
7. *Globorotalia truncatulinoides* (d'Orbigny) 95SLC17 40-50cm, spiral view
8. *Globorotalia truncatulinoides* (d'Orbigny) 95SLC15, umbilical view

Fig. 5-7-1 (1) Photographs of microscopic observation of microfossils

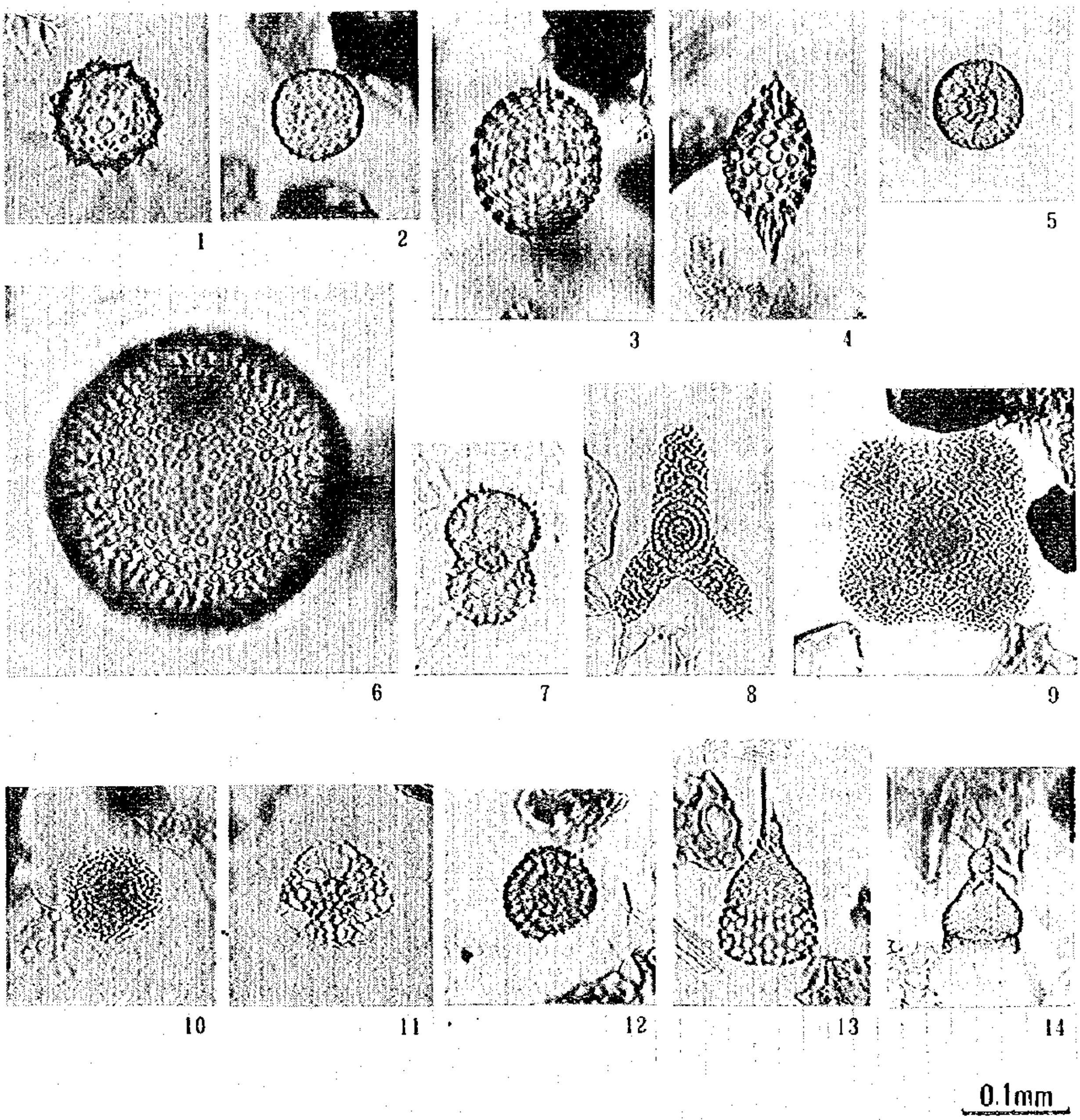

(Radiolaria)

1. Acrosphaera spinosa (95SFPG02)
2. Siphonosphaera sp. (95SFPG01)
3. Axoprunum stauraxonium (95SFPG02)
4. Ellipsoxiphus atractus (95SLC17)
5. Heliosphaera inermis (95SFPG02)
6. Cenosphaera sp. (95SLC15F)
7. Didymocyrtis tetrathalamus (95SFPG02)
8. Euchitonia furcata (95SFPG02)
9. Spongaster tetras tetras (95SFPG01)
10. Spongodiscidae gen. et sp. indet. (95SFPG02)
11. Hexapyle sp. (95SFPG02)
12. Lithelius minor (95SFPG02)
13. Lamprocyclas maritalis (95SLC15F)
14. Theocorythium trachelium (95SFPG02)

Fig. 5-7-1 (2) Photographs of microscopic observation of microfossils

Globigerinoides sacculifer, it belongs to tropical or subtropical area.

(2) Radiolaria

In all four samples, radiolarians are very rare and poor in species number. No diagnostic radiolarians provide precise information on the geological age. Rare occurrence of radiolarians suggests that organic particles such as radiolarians were diluted by a very high sedimentation rate.

1) 95SFPG01F (See Fig. 4-1-2 (4))

Radiolarians are moderately preserved. Little corrosion of the surface of shells is observed. The species of radiolarians are mainly *Acrosphaera spinosa* (Haeckel), *Axoprunum stauraxonium* Haeckel and *Spongaster tetras tetras* Ehrenberg, which live in today's tropical and subtropical regions.

2) 95SFPG02F (See Fig. 4-1-2 (4))

Radiolarians are moderately preserved. Little corrosion of the surface of shells is observed. The species of radiolarians are mainly *Acrosphaera spinosa*, *Axoprunum stauraxonium*, *Didymocyrtis tetrathalamus* (Haeckel) and *Theocorythium trachelium* (Ehrenberg), which live in today's tropical and subtropical regions.

3) 95SLC15F (See Fig. 4-1-2 (2))

Radiolarians are moderately preserved. Little corrosion of the surface of shells is observed. The species of radiolarians are mainly *Acrosphaera spinosa*, *Axoprunum stauraxonium* and *Theocorythium trachelium*, which live in today's tropical and subtropical regions.

4) 95SLC17F (See Fig. 4-1-2 (2))

Radiolarians are moderately preserved. Little corrosion of the surface of shells is observed. The species of radiolarians are mainly *Axoprunum stauraxonium* and *Ellipsoxiphus atractus* Haeckel, which live in today's tropical and subtropical regions. These possess stout spherical or ellipsoidal shells. Other species having relatively fragile shells such as *Acrosphaera spinosa*, which is dominant in other samples, are not observed. This fact suggests the sorting by a bottom current or the destruction of shells by the friction with volcanic ash particles.

(3) Conclusions

In all four samples, foraminiferas and radiolarians are composed of the species occurring in the tropical to subtropical regions. The sample of 95SFPG01, which locates in the southmost survey area, namely in higher latitude area, actually includes the foraminifera which is common in the middle latitude area.

CHAPTER 6 DISCUSSION

In Lau Basin which is the current spreading back−arc basin, Mariana Trough, North Fiji Basin, Okinawa Trough and so on, active hydrothermal activities or hydrothermal deposits are discovered. All these hydrothermal activities occur in the spreading center of the basin.

In the Lau back−arc basin, high temperature active chimneys and sulfide ore deposits are confirmed on the southernmost part of the Valu Fa Ridge which is an active spreading center. The survey area includes a part of this hydrothermal activity area in the southern part of the area, and almost part of the Valu Fa Ridge with the northern extension of the ridge as its center.

Thus, the survey area is expected to have an enough potential for hydrothermal activity. As a result of survey, however, neither hydrothermal activity, hydrothermal ore deposits nor their indications are found. Although several precipitations of manganese oxides and iron oxides are confirmed, these precipitations are not the evidence suggesting the typical hydrothermal activities. It is the known ore deposits district that shows the most sites of the ore indications.

Judging from the geological structure of the spreading center, the survey area is roughly divided into two areas in north and south. In the south the spreading center generally forms ridges, while grabens in the north.

In the ridges of the southern part of the area, brecciated lava, aa lava and pillow breccia of basalt are predominant so that much sea water penetrates into gaps (between pebbles) of lava. Under such circumstances, the hydrothermal fluids coming up from the underground mix with cold sea water and cool down, which makes hydrothermal activity hard to come up to the sea floor. From the topographic factor, in steep ridges sea water easily penetrates into the deeper part from the surface.

In the grabens of the northern part of the area, open cracks formed by tension stress field due to the spreading are very abundant. It is conceivable that much sea water seeps into the basement rock through these cracks.

In the survey area, therefore, the shallow parts of outcropping basement rocks form generally a discharged zone. The condition that hydrothermal deposits occur in such circumstances is the existence of strong hydrothermal activity as well as a cap rock sealing it in any forms. In the case of the known ore deposits in the southern end of the Valu Fa Ridge, iron−manganese crusts formed by the hydrothermal activity play a roll of cap rock, and chimneys and ore deposits occur along the normal fault made by a tectonic movement.

In this survey, we investigated first around this known hydrothermal ore deposits, and then, considering these results and existing data such as literature, we carried out the survey preferentially in the places which have characteristics of geographical and geological stuctures and which are expected to have a high potential of ore deposits. Bacause the sea floor sediments in the northern spreading center of the survey area are more thickly deposited than those in the southern spreading center, and so on, the volcanic activity of the northern area is judged to be old and inactive. In the southmost part of the Valu Fa Ridge (outside the survey area) where the spreading center is propagating towards south, the volcanic activity is continuously occurring. From these facts, it is concluded that the potential of ore deposits is low in the northern part of the survey area and high in the spreading ridge of the southern part.

CHAPTER 7 CONCLUSION

The survey has been undertaken for five year period starting from fiscal 1995. The survey of the first year, consisting of bathymetric survey and exploration of submarine hydrothermal ore deposit, was carried out within the exclusive economic zone of the Kingdom of Tonga. The actual survey period is 69 days.

The survey area locates in the middle to eastern part of the Lau Basin in the west of Tonga Islands. In the Lau Basin, there are two spreading centers running NNE–SSW direction in the central part of the northern area and the eastern part of the southern area. The southern spreading center (Valu Fa Ridge) runs through in the center of the survey area.

The survey consists of bathymetric survey by MBES to make a bathymetric map, SSS survey, sea floor observation by FDC, and sampling by LC, FPG and CB for ore deposits survey. Moreover, as a supplementary survey for geological survey, magnetic survey was carried out simultaneously with the bathymetric survey. Water temperature measurements using CTD mounted on FDC were also made.

(Bathymetric Survey)

The basic track line interval of bathymetric survey is 2 nautical miles with a supplementary line interval of 1 nautical mile in a shallow area. A total line length is 6,060.6 nautical miles.

According to the bathymetric map, detail topography of the whole survey area and the spreading center running NNE–SSW direction in the middle of the survey area are clarified, confirming some characteristic topography which suggests the tectonic movement. The spreading center running through the area consists of several grabens and ridges, and the overlapping spreading center was detected in the center of the area.

(MBES Acoustic Reflection Image)

The acoustic reflection image was made in receiving sound echo from each beam by MBES. This image is useful to clarify the status of sediments to some extent by the strength of acoustic reflection such as high sound echo from the outcrops and low sound echo from thick sediments. Thus, acoustic reflection image is used for distribution of sediments, and is effective data for selecting FDC observation sites and sampling points.

In the survey area, high sonic pressure zone which corresponds to NNE–SSW trending spreading center was clearly detected by MBES acoustic reflection image.

(SSS Survey)

The object of the SSS survey is to study precise topography and distribution of sediments, and to select the site for sea floor observation of FDC. Three survey lines were established around the spreading center in the central part of the area. Total line length is 49.7 nautical miles. The SSS records show linear structures which suggest cracks of rocks, topographic high in the form of a mound, and images which suggest widely distributed outcrops. Furthermore, the detailed distributions of sea floor sediments were clarified, which provide the important information for selecting sea floor observation sites. The records, which might be a plume and a direct sign of hydrothermal activity, were shown in several places.

(nSBP Survey)

The objects of nSBP survey are to know the distribution of sea floor sediments and under-sea floor structure. As a result of the survey, submarine structures such as distributions of sediments, etc. were considerably clarified, corresponding well with sounding image map. An application limit, however, is found in the area of steep slope, so that this method could be applied as a supplementary tool for hydrothermal exploration.

(Magnetic Survey)

As shown in the total magnetic force map, the total magnetic intensity in the survey area is within the range of 42,300 – 44,800 nT, gradually increasing towards the south as a general tendency. This local gradient is concordant with the theoretical global magnetic field.

As seen in the IGRF residual magnetic anomaly map, amplitude of anomaly is rather small within the range of −300 – +300 nT, and the NNE−SSW trending magnetic anomalous belt is predominant in all over the area, which correspond well with topographic trend of the survey area.

As the results of magnetic analysis, several high magnetization belts are detected in "the positive magnetization dominant area". Most of these belts correspond to the ridges. Especially, high magnetization zone in the central part of "the positive magnetization dominant area" is continuous corresponding to the ridges, which are considered to be the spreading center. Furthermore, judging from the characteristics of distribution of positive magnetization dominant area in the northern and southern parts, it is estimated that spreading rate increases towards the north or beginning age of spreading may be earlier in the northern part than that in the southern part.

(Geological Structure)

The most important and predominant geological structure is the spreading center of the Lau Basin, which runs NNE−SSW direction in the survey area. This spreading center consists of several ridges and grabens in echelon array, and in the center of the area overlapping spreading centers are observed at two places. The spreading center in the northern half of the area is formed mainly by grabens, while the southern spreading center by ridges.

The NNE−SSW trending lineaments in parallel with the spreading center is predominant, and near the overlapping spreading center or the bended zone, the parallel lineaments with these spreading center are observed. Most of the lineaments mean the cliff of normal fault formed by the spreading movement.

(Ore Deposits Investigation)

As a part of ore deposits investigation, FDC survey, SSS survey, and sampling by LC, FPG and CB were conducted. The surveys were mostly focused to the spreading center where the latest volcanic rocks existed.

Firstly, the sea floor observation was made by FDC survey to study the characteristics of volcanic products, muddy sediments and geological structures and to find out ore deposits. The SSS survey was made in a restricted area as a supplement. Then, samplings were carried out based on these survey results.

(FDC Survey)

In the middle to southern part of the area, 10 track lines were set to run along or across the spreading center, and in the southern part of the area, two track lines were set over the knolls in the east of the spreading center and one on the seamount in the west of it, with 13 track lines in total.

As a result, only local precipitations of manganese oxides and iron oxides are confirmed as weak ore indications in several places. No hydrothermal ore deposits, hydrothermal activity, even nor their significant signs were found out.

(Temperature Anomaly)

On−line temperature measurements were carried out by CTD which is mounted on FDC over all the FDC survey lines.

Several temperature anomalies were detected on 6 track lines. Some of them show the values which could suggest the sign of hydrothermal activity, on the contrary, no eminent anomaly is detected in the FDC observations.

(Sampling)

In the northern part of the survey area, LC sampling was made at 17 stations in the graben of the spreading center and its eastern side. In the central southern part of the area, LC sampling was also made at 14 stations along the baseline crossing the spreading ridge. Collection rate of sediments was very poor on the spreading center because of no sediments or thin sediments, but much better in other area. No ore indication such as argillization is observed in the sediments, but a few pyrites were confirmed in basalt fragments which were collected in two places.

FPG samplings were made at three places; the spreading center, the seamount and knoll chain in the southernmost part of the area. At each site, basalt consisting mainly of pillow lava were collected.

CB samplings were conducted at 11 places around the spreading center in the central to northern part of the area. The target of sampling was set to the fault cliffs corresponding to the boundary between grabens and horsts. As a result, basalt consisting mainly of pillow lava were collected at 8 stations.

Many basalt lava were collected by FPG and CB, but no ore indications such as mineralization and alteration were observed.

(Discussions)

As procedure of the actual survey, we firstly made a bathymetric map simultaneously with magnetic map, and on the basis of these and the potential place of known ore deposit, promising areas were selected. After this, the sea floor observation by FDC and the investigation of precise topography and sea floor situation by SSS in some area were made, and the sampling locations were determined. The results of the MBES acoustic reflection image can be used for the estimation how sediments cover the sea floor, so these are useful in selecting outcropped zone.

The survey area includes almost all the Valu Fa Ridge except for its southmost part, which is a current spreading center. The existence of active hydrothermal activities and ore deposits in the southmost part of Valu Fa Ridge was reported. The survey area includes the north end of these ore deposits and corresponds to the northern extension area of the deposits, so that we expected ore deposits to exist in the survey area. In this survey, however, hydrothermal activity, hydrothermal ore deposits and their significant indications were not observed at all.

The biggest reason no hydrothermal ore deposits were observed is presumed that the cap rock sealing the hydrothermal activity has not been formed because the hydrothermal activity has been weak and not been continuous. This presumption is based on the fact that we could find out no hydrothermal activities and hydrothermal ore deposits by the sea floor observations and samplings although young volcanic activities exist, and that the ore indications such as temperature anomalies are local and very weak.

Considering the occurrence condition of the known ore deposits, in this survey we carried out the investigation preferentially in the places which have characteristics of geographical and geological structures. Judging from the results of this investigation and the past investigations around this survey area, we concluded that the potential of ore deposits is low in the northern part of the survey area and high in the spreading ridge of the southern part.

[References]

Be, A.W.H., An Ecological Zoogeographic and Taxonomic Review of Recent Planktonic Foraminifera. in Ramsay, A. T. S. (ed.), Oceanoc Micropaleontology. London, Academic Press, v.1, p.1–100, 1977.

Berggren, W.A., Kent, D.V., Flynn, J.J., and van Couvering, J.A., Cenozoic Geochronology, Geol. Soc. Am. Bull., v.96, p.1407–1418, 1985.

Blow, W.H., Late Middle Eocene to Recent Planktonic Foraminiferal Biostratigraphy. in Bronniman, P. and Renz, H.H. (ed.), Proc. 1st Int. Conf.Planktonic Microfossils, Genova, 1967, Leiden (EJ. Brill), v.1, p.199–422, 1969.

Carbotte, S. and Macdonald, K., East Pacific Rise 8° –10° 30'N, Evolution of ridge segments and discontinuities from SeaMARCII and three–dimensional magnetic studies, Journal of geophysical research, Vol.97,No.B5, p.6959–6982, 1992.

Cordell, L. and Henderson, R.G., Iterative Three–dimensional solution of gravity anomaly data using a digital computer, Geophysics, Vol.33, 1968.

Evensen, N.M.,Hamilton, P.J. and O'Nions, R.K., Rare–earth Abundances in Chondritic meteorites, Geochim. Cosmochim. Acta, v.42, p.1199–1212, 1978.

Fouquet, Y., von Stackelberg, U., Charlou, J.L., Erzinger, J., Herzig, P.M., Muhe, R., and Wiedicke, M., Metallogenesis in Back–Arc Environments : The Lau Basin Example, Economic Geology, v. 88, p. 2154–2181, 1993.

Ghaproniere, G.C.H. and Nishi, H., Miocene to Pleistocene Planktonic Foraminifer Biostratigraphy of the Lau Basin and Tongan Platform, Leg 135, Proceedings of the Ocean Drilling Program, Scientific Results, v. 135, p.207–229, 1994.

Ghaproniere, G.C.H., Styzen, M.J., Sager, W.W., Nishi, H., Quinterno, P.J., and Abrahamsen, N., Late Neogene Biostratigraphic and magnetostratigraphic Synthesis, Leg 135, Proceedings of the Ocean Drilling Program, Scientific Results, v. 135, p.857–877, 1994.

Hawkins, J.W. and Melchior, J.T., Petrology of Mariana Trough and Lau Basin Basalts, Journal of Geophysical Research, v. 90, p. 11431–11468, 1985.

Herzig, P.M., Hannington, M.D., Fouquet, Y., von Stackelberg, U., and Petersen, S., Gold–Rich Polymetallic Sulfides from the Lau Back Arc and Implications for the Geochemistry of Gold in Sea–Floor Hydrothermal Systems of the Southwest Pacific, Economic Geology, v. 88, p. 2182–2209, 1993.

Martinez, F., Fryer, P., Baker .N.A. and Yamazaki, T., Evolution of backarc rifting:Mariana Trough, 20–24 N, Journal of geophysical research, Vol.100,No.B3, p.3807–3827, 1995.

Meshede, A Method of Discriminating between Different Types of Mid-ocean Ridge Basalts and Continental Tholleites with the Nb-Zr-Y Diagram, Chem. Geol., v.56, p.207-218, 1986.

Middlemost, The Basalt Clan, Earth Sci. Rev., v.11, p.337-364, 1975.

Mullen, E.D., $MnO/TiO_2/P_2O_5$; A Minor Element Discriminant for Basaltic Rocks of Oceanic Environments and its Implication for Petrogenesis, Earth Planet. Sci. Lett., v.62, p.53-62, 1983.

Spector, A. and Grant, F.S., Statistical models for interpreting aero-magnetic data, Geophysics, Vol.35, 1970.

Steiger, R. and Jaeger, E., Subcommision on geochronology, Convention on the use of decay constants in geo- and cosmo-chronology, Earth Planet. Sci. Let., v.36, p.359-362, 1977.

Wiedicke, M. and Collier, J., Morphology of the Valu Fa Spreading Ridge in the Southern Lau Basin, Journal of Geophysical Research, v. 98, p. 11769-11782, 1993.

Wiedicke, M. and Habler, W., Morphotectonic Characteristics of a Propagating Spreading System in the Northern Lau Basin, Journal of Geophysical Research, v. 98, p. 11783-11797, 1993.

Wilson, M., Igneous Petrogenesis -- A Global Tectonic Approach, Unwim Hyman, London, 466p, 1989.

[APPENDIX]

APPENDIX Table 1 Results of FDC survey

Track line No.	Item	Observation		Location		Depth	Obs. time	Obs. length	Number of
		Date	Time	Latitude (S)	Longitude (W)	(m)	(SO to EO)	(nm)	photographs
	TS	8/8	19:05						
95SFDC01	SO		19:44	21° 50.60'	176° 29.77'	1,986			
	EO	8/9	01:35	21° 56.30'	176° 32.29'	1,829	5h 51m	6.2	300
	TD		02:16						
	TS	8/12	18:56						
95SFDC02	SO		19:54	20° 20.22'	176° 07.71'	2,771			
	EO		22:47	20° 22.31'	176° 08.93'	2,651	2h 53m	2.4	126
	TD		23:37						
	TS	8/13	00:03						
95SFDC03	SO		00:55	20° 25.32'	176° 10.99'	2,602			
	EO		03:47	20° 26.49'	176° 08.82'	2,585	2h 52m	2.4	124
	TD		04:36						
	TS	8/13	19:02						
95SFDC04	SO		19:58	20° 31.01'	176° 11.29'	2,676			
	EO		21:35	20° 29.64'	176° 10.91'	2,732	1h 37m	1.4	62
	TD		22:30						
	TS	8/13	23:00						
95SFDC05	SO		23:56	20° 30.76'	176° 11.53'	2,744			
	EO	8/14	01:28	20° 29.41'	176° 10.98'	2,742	1h 32m	1.4	94
	TD		02:23						
	TS	8/14	18:58						
95SFDC06	SO		19:50	20° 27.03'	176° 10.03'	2,610			
	EO		20:50	20° 27.11'	176° 09.29'	2,578	1h 00m	0.7	36
	TD		21:40						
	TS	8/14	22:28						
95SFDC07	SO		23:19	20° 32.39'	176° 12.97'	2,555			
	EO	8/15	04:06	20° 33.11'	176° 08.07'	2,331	4h 47m	4.7	213
	TD		04:54						
	TS	8/15	19:06						
95SFDC08	SO		19:48	21° 24.75'	176° 24.66'	1,986			
	EO		23:28	21° 24.77'	176° 21.05'	2,213	3h 40m	3.4	148
	TD	8/16	00:15						
	TS	8/17	09:03						
95SFDC09	SO		19:54	21° 50.91'	176° 46.63'	2,267			
	EO	8/18	01:54	21° 56.41'	176° 43.41'	1,527	6h 00m	6.3	307
	TD		02:30						
	TS	8/18	19:03						
95SFDC10	SO		19:48	21° 23.15'	176° 16.14'	2,146			
	EO		23:12	21° 26.48'	176° 16.39'	2,424	3h 24m	3.3	135
	TD	8/19	00:00						
	TS	8/19	01:02						
95SFDC11	SO		02:33	21° 34.12'	176° 19.83'	2,477			
	EO		03:47	21° 34.79'	176° 18.65'	2,266	1h 14m	1.3	53
	TD		04:34						
	TS	8/19	18:30						
95SFDC12	SO		19:15	21° 17.69'	176° 21.63'	2,122			
	EO		20:52	21° 16.47'	176° 20.17'	2,087	1h 37m	1.8	77
	TD		21:35						
	TS	8/20	23:57						
95SFDC13	SO		00:43	20° 53.21'	176° 14.17'	2,239			
	EO		02:56	20° 52.70'	176° 12.02'	2,166	2h 13m	2.1	155
	TD		03:40						

Legend of Item : TS : FDC on the sea surface SO : start of the observation EO : end of the observation TD : FDC on the de

Note : Date and Time show UTC.

Depth is calculated by CTD data, and Location by wire length and Depth.

APPENDIX Table 2 (1) Results of sampling survey

Sample No.	Date	Time	Longitude	Latitude	Depth	Core Length	Remarks
95SLC01	7/27	19:52:25	21° 04.901'S	176° 16.849'W	2,296m	0cm	*1,*2
95SLC02	7/27	21:54:55	21° 03.732'S	176° 16.212'W	2,436m	0cm	*1,*2
95SLC03	7/27	23:49:20	21° 03.701'S	176° 15.333'W	2,126m	110cm	
95SLC04	7/28	01:50:30	21° 05.298'S	176° 15.977'W	2,128m	95cm	*1
95SLC05	7/28	21:12:50	21° 06.022'S	176° 12.050'W	2,447m	90cm	
95SLC06	7/28	23:12:25	21° 05.689'S	176° 13.778'W	2,330m	0cm	*1
95SLC07	7/29	01:08:10	21° 05.325'S	176° 14.258'W	2,401m	100cm	
95SLC08	7/29	03:05:50	21° 04.600'S	176° 13.985'W	2,309m	85cm	
95SLC09	7/28	19:10:35	21° 04.845'S	176° 15.080'W	2,211m	55cm	
95SLC10	7/29	19:16:25	21° 03.954'S	176° 17.194'W	2,152m	60cm	
95SLC11	7/29	21:14:10	21° 03.266'S	176° 17.650'W	2,342m	0cm	*1,*2
95SLC12	7/29	23:10:20	21° 02.870'S	176° 18.120'W	2,211m	0cm	*1,*3
95SLC13	7/30	01:12:45	21° 02.506'S	176° 19.533'W	2,456m	110cm	
95SLC14	7/30	04:04:50	21° 01.121'S	176° 20.074'W	2,259m	90cm	
95SLC15	8/22	20:13:45	20° 20.836'S	176° 08.063'W	2,809m	20cm	*1
95SLC16	8/22	22:40:05	20° 21.973'S	176° 08.593'W	2,792m	0cm	*1,*2
95SLC17	8/23	01:03:00	20° 23.495'S	176° 08.266'W	2,515m	93cm	*1
95SLC18	8/23	03:39:55	20° 26.071'S	176° 09.966'W	2,737m	0cm	*1,*2
95SLC19	8/23	19:34:25	20° 13.192'S	176° 05.298'W	2,796m	70cm	
95SLC20	8/23	22:20:25	20° 15.892'S	176° 06.835'W	2,275m	0cm	*1,*3
95SLC21	8/24	00:55:00	20° 18.011'S	176° 06.936'W	2,845m	105cm	*1
95SLC22	8/24	03:29:05	20° 19.973'S	176° 07.731'W	2,788m	0cm	*1,*2
95SLC23	8/24	19:31:10	19° 52.131'S	176° 03.383'W	2,626m	0cm	*1,*2
95SLC24	8/24	22:00:20	19° 53.907'S	176° 04.104'W	2,638m	0cm	*1,*2
95SLC25	8/25	00:33:35	19° 55.920'S	176° 04.761'W	2,719m	0cm	*1,*2
95SLC26	8/25	19:29:10	19° 46.543'S	175° 57.446'W	2,615m	200cm	
95SLC27	8/26	01:23:35	19° 36.004'S	175° 42.942'W	2,368m	215cm	
95SLC28	8/26	19:31:45	19° 49.326'S	175° 58.453'W	2,653m	255cm	
95SLC29	8/26	22:07:40	19° 49.006'S	175° 56.116'W	2,450m	285cm	
95SLC30	8/27	00:35:25	19° 49.011'S	175° 53.485'W	2,603m	165cm	
95SLC31	8/27	02:59:45	19° 46.669'S	175° 53.071'W	2,605m	155cm	

*1 : Bit was deformed

*2 : No sample was collected

*3 : Rock fragments were collected

APPENDIX Table 2 (2) Results of sampling survey

Sample No.	Item	Date	Time	Longitude	Latitude	Depth	Sample wt.	Remarks
95SFPG01	LF	8/20	20:33:05	21° 56.324'S	176° 43.781'W	1,657m	480kg	
95SFPG02	LF	8/21	00:11:30	21° 50.077'S	176° 29.184'W	1,910m	380kg	
95SFPG03	LF	8/21	03:37:50	21° 57.079'S	176° 22.118'W	2,061m	60kg	
95SCB01	SD	8/21	21:34:10	21° 02.562'S	176° 18.488'W	2,306m	3.9kg	
	ED		22:09:55	21° 02.956'S	176° 18.395'W	2,320m		
95SCB02	SD	8/22	00:37:30	21° 02.828'S	176° 18.202'W	2,276m	1.38kg	
	ED		01:18:50	21° 02.970'S	176° 17.871'W	2,306m		
95SCB03	SD	8/22	03:52:30	21° 08.924'S	176° 18.711'W	2,195m	65kg	
	ED		04:24:25	21° 09.219'S	176° 18.296'W	2,255m		
95SCB04	SD	8/27	19:26:50	20° 15.701'S	176° 06.990'W	2,743m	146kg	
	ED		20:01:25	20° 16.125'S	176° 06.570'W	2,755m		
95SCB05	SD	8/27	22:48:20	20° 21.178'S	176° 09.292'W	2,737m	210.92kg	
	ED		23:47:10	20° 21.970'S	176° 08.726'W	2,798m		
95SCB06	SD	8/28	02:18:40	20° 21.325'S	176° 07.907'W	2,717m	137.56kg	
	ED		02:58:05	20° 21.444'S	176° 07.663'W	2,540m		
95SCB07	SD	8/28	19:23:05	19° 55.015'S	176° 04.019'W	2,647m	410.05kg	
	ED		20:14:20	19° 55.426'S	176° 03.832'W	2,540m		
95SCB08	SD	8/28	23:02:30	19° 51.512'S	176° 02.904'W	2,566m	34.1kg	
	ED		23:36:50	19° 51.693'S	176° 02.340'W	2,556m		
95SCB09	SD	8/29	01:58:30	19° 51.892'S	175° 59.097'W	2,531m	12.2kg	
	ED		02:41:40	19° 52.151'S	175° 58.792'W	2,394m		
95SCB10	SD	8/29	19:23:45	19° 49.958'S	175° 54.953'W	2,563m	4.14kg	
	ED		20:25:55	19° 49.914'S	175° 54.008'W	2,520m		
95SCB11	SD	8/29	23:38:10	19° 50.531'S	175° 41.664'W	2,023m	1.3kg	
	ED	8/30	00:22:25	19° 50.822'S	175° 41.369'W	1,915m		

Legend of Item : LF : leave the sea floor SD : start of dredge ED : end of dredge

Note : Date and Time show UTC. Longitude and Latitude are the GPS position of R/V.

Depth data of LC (except for LC24,LC26-30) and CB08-11 are calculated by CTD data.

The other Depth data are NBS data.

Sample wt. means the total weight of rocks and sediments.

APPENDIX Table 3 Ore Indications

Sampling No. Track line No.		Location Latitude / Longitude	Depth (m)	Time (UTC)	Range	Contents	Photo No.
95SLC12		21° 02.87′ S	2,211	—	unknown	Very weak dissemination	—
		176° 18.12′ W				of sulfides in basalt	
95SLC20		20° 15.89′ S	1,412	—	unknown	Weak dissemination	—
		176° 06.83′ W				of sulfides in basalt	
95SFDC01		21° 52.99′ S	1,773	22:21:55	partly	White materials in sediments	133
		176° 30.84′ W					
	from	21° 53.64′ S	1,795	23:00:25	a few 10m	Effusive holes and deposits	164-169
		176° 31.16′ W				of black Mn-oxides	
	to	21° 53.65′ S	1,786	23:01:15		Deposits of yellow to	
		176° 31.16′ W				yellowish brown oxides	
	from	21° 53.87′ S	1,846	23:14:40	a few 10m	Deposits of black Mn-oxides	176-178
		176° 31.33′ W				on the rock surface	
	to	21° 53.89′ S	1,845	23:15:30			
		176° 31.33′ W					
		21° 54.99′ S	1,895	00:20:00	partly	Deposits of brown oxides	227
		176° 31.75′ W				in the inside wall of pit	
	from	21° 56.09′ S	1,829	01:23:20	140m	Effusive holes and deposits	283-292
		176° 32.20′ W				of black Mn-oxides	
	to	21° 56.17′ S	1,835	01:28:05		Deposits of yellow to	
		176° 32.24′ W				yellowish brown oxides	
95SFDC02	from	20° 20.85′ S	2,791	20:49:45	spotty	Effusive holes and deposits	26-31
		176° 08.05′ W			within 100m	of black Mn-oxides	
	to	20° 20.91′ S	2,797	20:52:45		Deposits of yellowish brown	
		176° 08.07′ W				oxides	
95SFDC09		21° 55.92′ S	1,591	01:24:45	partly	Deposits of black Mn-oxides	290
		176° 43.66′ W			(widely?)		
95SFDC10	from	21° 23.68′ S	1,780	20:17:55	a few 10m	Deposits of yellowish brown	16-18
		176° 16.07′ W				oxides	
	to	21° 23.69′ S	1,783	20:18:55			
		176° 16.08′ W					
95SFDC12	from	21° 17.40′ S	2,093	19:47:25	about 10m	White materials and brown	27,28
		176° 21.17′ W				oxides on the rock surface	
	to	21° 17.40′ S	2,097	19:47:40			
		176° 21.17′ W					
	from	21° 17.32′ S	2,074	19:52:15	50m	White materials on the	32-34
		176° 21.10′ W				rock surface	
	to	21° 17.29′ S	2,058	19:54:20		Deposits of brown materials	
		176° 21.08′ W					
95SFDC13		20° 53.19′ S	2,203	00:52:20	partly	White materials on the	6
		176° 14.06′ W				rock surface	

APPENDIX Table 4 (1) Sample list of analysis and observation (sediments)

Sample No.	Latitude (S) (deg.)	(min.)	Longitude (W) (deg.)	(min.)	Depth (m)	Sampling depth (cm) top	bottom	Sediments Munsell No. & Color	Size	Analysis M	C	F
95SLC03-M1	21	03.701	176	15.333	2,126	5	10	10YR4/2 dark grayish brown	silt	O		
-M2						45	50	5Y4/4 olive	silt	O		
-M3						70	75	10YR5/2 grayish brown	silt	O		
-M4						100	105	2.5Y3/2 very dark grayish brown	silt	O		
95SLC04-M1	21	05.298	176	15.997	2,128	5	10	10YR3/2 very dark grayish brown	silt	O		
-M2						35	40	10YR2/2 very dark brown	silt	O		
-M3						55	60	5Y5/3 olive	silt	O		
-M4						80	85	10YR3/2 very dark grayish brown	silt	O		
95SLC05-M1	21	06.022	176	12.050	2,447	5	10	10YR3/2 very dark grayish brown	silt	O		
-M2						20	25	2.5Y4/0 dark gray	silt	O		
-M3						35	40	10YR3/2 very dark grayish brown	silt	O		
-M4						65	70	5Y2.5/1 black	silt	O		
-M5						80	85	5Y3/2 dark olive gray	silt	O		
95SLC07-M1	21	05.325	176	14.258	2,401	0	5	10YR3/3 dark brown	silt	O		
-M2						35	40	5Y4/3 olive	silt	O		
-M3						70	75	2.5Y3/2 very dark grayish brown	silt	O		
-M4						90	95	5Y2.5/1 black	silt	O		
95SLC08-M1	21	04.600	176	13.985	2,309	0	5	10YR3/2 very dark grayish brown	silt	O		
-M2						15	20	10YR3/1 very dark gray	silt	O		
-M3						55	60	5Y2.5/1 black	silt	O		
-C1						60	65	10YR2/1 black	sand		O	
-M4						65	70	5YR2.5/2 dark reddish brown	silt	O		
-M5						80	85	10YR4/2 dark grayish brown	silt	O		
95SLC09-M1	21	04.845	176	15.080	2,211	5	10	2.5Y3/2 very dark grayish brown	silt	O		
-M2						50	55	5Y3/2 dark olive gray	silt	O		
95SLC10-M1	21	03.954	176	17.194	2,152	5	10	10YR3/2 very dark grayish brown	silt	O		
-C1						15	20	10YR2/1 black	sand		O	
-M2						25	30	10YR3/2 very dark grayish brown	silt	O		
-M3						35	40	10YR2/2 very dark brown	silt	O		
-C2						40	45	10YR2/1 black	sand		O	
-M4						55	60	5YR3/1 very dark gray	silt	O		
95SLC13-M1	21	02.506	176	19.533	2,456	5	10	5YR3/1 very dark gray	silt	O		
-M2						25	30	2.5Y3/2 very dark grayish brown	silt	O		
-C1						60	65	5Y2.5/1 black	sand		O	
-M3						65	70	5Y2.5/1 black	sand	O		
-M4						80	85	10YR2/2 very dark brown	silt	O		
-C2						100	105	5Y2.5/1 black	sand		O	
-M5						105	110	5YR3/1 very dark gray	silt	O		
95SLC14-M1	21	01.121	176	20.074	2,259	5	10	10YR3/2 very dark grayish brown	silt	O		
-C1						15	20	10YR2/1 black	sand		O	
-M2						25	30	10YR3/2 very dark grayish brown	silt	O		
-M3						35	40	10YR3/2 very dark grayish brown	silt	O		
-M4						50	55	10YR3/2 very dark grayish brown	silt	O		
-M5						80	85	2.5Y4/2 dark grayish brown	silt	O		
95SLC15-M1	20	20.836	176	08.063	2,799	5	10	10YR3/3 dark brown	silt	O		
-F						10	15	10YR3/3 dark brown	silt			O
-M2						15	20	7.5YR4/0 dark gray	silt	O		
95SLC17-M1	20	23.495	176	08.266	2,515	5	10	10YR3/3 dark brown	silt	O		
-M2						30	35	10YR3/3 dark brown	silt	O		
-F						40	50	10YR2/1 black	sand			O
-M3						50	55	10YR3/3 dark brown	silt	O		
-M4						80	85	10YR3/2 very dark grayish brown	silt	O		

APPENDIX Table 4 (2) Sample list of analysis and observation (sediments)

Sample No.	Latitude (S)		Longitude (W)		Depth	Sampling depth		Sediments		Analysis		
	(deg.)	(min.)	(deg.)	(min.)	(m)	(cm) top	bottom	Munsell No. & Color	Size	M	C	F
95SLC19-M1	20	13.192	176	05.298	2,796	10	15	10YR3/3 dark brown	silt	○		
-M2						30	35	5Y4/1 dark gray	silt	○		
-M3						45	50	5Y4/1 dark gray	silt	○		
-M4						65	70	5Y4/1 dark gray	silt	○		
95SLC21-M1	20	18.011	176	06.936	2,845	5	10	10YR3/3 dark brown	silt	○		
-M2						25	30	10YR3/2 very dark grayish brown	silt	○		
-M3						45	50	10YR3/2 very dark grayish brown	silt	○		
-M4						70	75	2.5Y3/2 very dark grayish brown	silt	○		
-M5						90	95	5Y4/2 olive gray	silt	○		
95SLC26-M1	19	46.543	175	57.466	2,615	10	15	10YR3/2 very dark grayish brown	silt	○		
-M2						30	35	10YR3/2 very dark grayish brown	silt	○		
-M3						45	50	10YR3/1 very dark gray	silt	○		
-M4						65	70	10YR3/2 very dark grayish brown	silt	○		
-M5						90	95	2.5Y4/2 dark grayish brown	silt	○		
-M6						110	115	10YR3/2 very dark grayish brown	silt	○		
-M7						125	130	10YR3/1 very dark gray	silt	○		
-M8						155	160	5Y5/2 olive gray	silt	○		
-M9						170	175	5Y5/3 olive	silt	○		
-M10						190	195	10YR3/2 very dark grayish brown	silt	○		
95SLC27-M1	19	36.004	175	42.942	2,368	5	10	10YR3/3 dark brown	silt	○		
-M2						20	25	10YR3/2 very dark grayish brown	silt	○		
-M3						35	40	10YR3/3 dark brown	silt	○		
-M4						70	75	10YR3/2 very dark grayish brown	silt	○		
-M5						95	100	10YR3/2 very dark grayish brown	silt	○		
-M6						125	130	5Y3/2 dark olive gray	silt	○		
-M7						155	160	2.5Y6/2 light brownish gray	silt	○		
-M8						170	175	2.5Y5/2 grayish brown	silt	○		
-M9						185	190	5Y3/2 dark olive gray	silt	○		
-M10						205	210	5Y2.5/1 black	silt	○		
95SLC28-M1	19	49.326	175	58.453	2,653	5	10	10YR3/3 dark brown	silt	○		
-M2						15	20	10YR3/2 very dark grayish brown	silt	○		
-M3						45	50	2.5Y3/2 very dark grayish brown	silt	○		
-M4						70	75	5Y3/2 dark olive gray	silt	○		
-M5						85	90	5Y2.5/2 black	silt	○		
-M6						105	110	2.5Y3/2 very dark grayish brown	silt	○		
-M7						135	140	5Y3/2 dark olive gray	silt	○		
-M8						160	165	5Y2.5/2 black	silt	○		
-M9						180	185	2.5Y3/2 very dark grayish brown	silt	○		
-M10						205	210	10YR3/2 very dark grayish brown	silt	○		
-M11						230	235	10YR3/2 very dark grayish brown	silt	○		
-M12						250	255	2.5Y4/2 dark grayish brown	silt	○		
95SLC29-M1	19	49.006	175	56.116	2,450	0	5	10YR3/3 dark brown	silt	○		
-M2						5	15	10YR3/2 very dark grayish brown	silt	○		
-M3						15	25	10YR3/2 very dark grayish brown	silt	○		
-M4						25	35	10YR3/2 very dark grayish brown	silt	○		
-M5						35	45	10YR3/2 very dark grayish brown	silt	○		
-M6						45	55	10YR3/3 dark brown	silt	○		
-M7						55	65	10YR2/2 very dark brown	silt	○		
-M8						65	75	10YR4/2 dark grayish brown	silt	○		
-M9						75	85	10YR4/2 dark grayish brown	silt	○		
-M10						85	95	10YR3/2 very dark grayish brown	sand	○		

APPENDIX Table 4 (3) Sample list of analysis and observation (sediments)

Sample No.	Latitude (S) (deg.)	Latitude (S) (min.)	Longitude (W) (deg.)	Longitude (W) (min.)	Depth (m)	Sampling depth (cm) top	Sampling depth bottom	Sediments Munsell No. & Color	Size	Analysis M	C	F
95SLC29-M11	19	49.006	175	56.116	2,450	95	105	5Y6/2 light olive gray	silt	○		
-M12						105	115	10YR3/2 very dark grayish brown	silt	○		
-M13						115	125	5Y4/2 olive gray	silt	○		
-M14						125	135	5Y4/2 olive gray	silt	○		
-M15						135	145	5Y4/2 olive gray	silt	○		
-M16						145	155	10YR3/2 very dark grayish brown	silt	○		
-M17						155	165	5Y2.5/2 black	silt	○		
-M18						165	175	10YR3/2 very dark grayish brown	silt	○		
-M19						175	185	10YR3/2 very dark grayish brown	silt	○		
-M20						185	195	2.5Y3/2 very dark grayish brown	silt	○		
-M21						195	205	10YR3/2 very dark grayish brown	silt	○		
-M22						205	215	10YR3/2 very dark grayish brown	silt	○		
-M23						215	225	2.5Y3/2 very dark grayish brown	silt	○		
-M24						225	235	2.5Y3/2 very dark grayish brown	silt	○		
-M25						235	245	10YR3/2 very dark grayish brown	silt	○		
-M26						245	255	10YR3/2 very dark grayish brown	silt	○		
-M27						255	265	10YR3/2 very dark grayish brown	silt	○		
-M28						265	275	2.5Y3/2 very dark grayish brown	silt	○		
-M29						275	285	2.5Y4/2 dark grayish brown	silt	○		
95SLC30-M1	19	49.011	175	53.485	2,603	5	10	2.5Y3/2 very dark grayish brown	silt	○		
-M2						25	30	10YR3/2 very dark grayish brown	silt	○		
-M3						50	55	10YR3/2 very dark grayish brown	silt	○		
-M4						65	70	10YR3/2 very dark grayish brown	silt	○		
-M5						80	85	5Y3/2 dark olive gray	silt	○		
-M6						105	110	10YR3/2 very dark grayish brown	silt	○		
-M7						145	150	2.5Y4/2 dark grayish brown	silt	○		
-M8						155	160	10YR3/2 very dark grayish brown	silt	○		
95SLC31-M1	19	46.669	175	53.071	2,605	5	10	2.5Y3/2 very dark grayish brown	silt	○		
-M2						25	30	10YR3/2 very dark grayish brown	silt	○		
-M3						45	50	10YR3/2 very dark grayish brown	silt	○		
-M4						70	75	10YR3/2 very dark grayish brown	silt	○		
-M5						95	100	10YR3/2 very dark grayish brown	silt	○		
-M6						115	120	2.5Y3/2 very dark grayish brown	silt	○		
-M7						135	140	5Y4/2 black	silt	○		
-M8						145	150	10YR3/2 very dark grayish brown	silt	○		
95SFPG01-M	21	56.324	176	43.781	1,657			very dark grayish brown	silt	○		
-F								very dark grayish brown	silt			○
95SFPG02-M	21	50.077	176	29.220	1,910			very dark grayish brown	silt	○		
-F								very dark grayish brown	silt			○
95SCB01-M	*		*					very dark grayish brown	silt	○		
95SCB02-M	*		*					very dark grayish brown	silt	○		
95SCB03-M	*		*					very dark grayish brown	silt	○		
95SCB05-M	*		*					very dark grayish brown	silt	○		
95SCB06-M	*		*					very dark grayish brown	silt	○		
95SCB07-M	*		*					very dark grayish brown	silt	○		
95SCB09-M	*		*					very dark grayish brown	silt	○		
95SCB10-M	*		*					very dark grayish brown	silt	○		
95SCB11-M	*		*					very dark grayish brown	silt	○		

APPENDIX Table 4 (4) Sample list of analysis and observation (rocks)

Sample No.	Latitude (S)		Longitude (W)		Depth	Rock facies	Analysis						
	(deg.)	(min.)	(deg.)	(min.)	(m)		C	M	N	T	P	X	K
95SLC12-M	21	02.870	176	18.120	2,211	basalt lava		○					
-T						basalt lava				○			
-P						basalt lava					○		
-X						basalt lava						○	
95SLC20-R	20	15.892	176	06.835	3,275	basalt lava	○	○	○				
-T						basalt lava				○			
-P						basalt lava					○		
-X						basalt lava						○	
-C+N						basalt lava (glass)	○		○				
95SFPG01-R	21	56.324	176	43.781	1,657	basalt lava	○	○	○				
-T						basalt lava				○			
-K						basalt lava							○
95SFPG02-R	21	50.077	176	29.184	1,910	basalt lava	○	○	○				
-T						basalt lava				○			
-X						basalt lava						○	
-K						basalt lava							○
-M+N						basalt lava (oxidized)		○	○				
95SFPG03-R	21	57.079	176	22.118	2,061	basalt lava	○	○	○				
-T1						basalt lava				○			
-T2						basalt lava				○			
-K						basalt lava							○
95SCB03-R1	*		*			basalt lava	○	○	○				
-R2						basalt lava (glass)	○	○	○				
-T						basalt lava				○			
-K						basalt lava							○
95SCB04-R1	*		*			basalt lava	○	○	○				
-R2						basalt lava (glass)	○	○	○				
-T						basalt lava				○			
-K						basalt lava							○
95SCB05-R1	*		*			basalt lava	○	○	○				
-R2						basalt lava (glass)	○	○	○				
-T1						basalt lava				○			
-T2						basalt lava				○			
-K						basalt lava							○
95SCB06-R	*		*			basalt lava	○	○	○				
-T						basalt lava				○			
-K						basalt lava							○
95SCB07-R1	*		*			basalt lava	○	○	○				
-R2						basalt lava (glass)	○	○	○				
-T1						basalt lava				○			
-T2						basalt lava				○			
-K						basalt lava							○
95SCB08-R	*		*			basalt lava	○	○	○				
-C+N						basalt lava (glass)	○		○				
-T						basalt lava				○			
-K						basalt lava							○
95SCB09-R	*		*			basalt lava	○	○	○				
-T						basalt lava				○			
-K						basalt lava							○
95SCB10-T	*		*			basalt lava				○			
95SCB11-T	*		*			basalt lava				○			

* : Locations of CB dredge sampling are shown in Appendix Table 2.

Legend of Analysis

C : Chemical analysis (major components)
M : Chemical analysis (base metal elements)
N : Chemical analysis (rare earth elements)
T : Thin section observation
P : Polish observation
X : X-ray diffraction analysis
K : Age determination (K-Ar method)
F : Micro fossil observation

Appendix Table 5 Sea-water sound velocity for MBES

19°16.5'S, 176°09.1'W (CTD01)		21°04.9'S, 176°17.0'W (LC01)	
Water depth (m)	Sound velocity (m/sec)	Water depth (m)	Sound velocity (m/sec)
10.0	1,535.9	10.0	1,532.6
20.0	1,536.4	20.0	1,532.5
40.0	1,536.8	40.0	1,533.1
60.0	1,536.2	60.0	1,533.3
80.0	1,535.0	80.0	1,533.6
100.0	1,532.1	100.0	1,533.6
150.0	1,528.3	150.0	1,529.1
200.0	1,525.5	200.0	1,526.7
300.0	1,516.5	300.0	1,519.6
400.0	1,503.5	400.0	1,510.2
500.0	1,492.6	500.0	1,498.2
600.0	1,488.5	600.0	1,489.2
700.0	1,486.3	700.0	1,485.8
800.0	1,485.4	800.0	1,483.9
1,000.0	1,484.5	1,000.0	1,482.8
1,500.0	1,485.6	1,501.0	1,485.2
2,001.0	1,492.4	2,000.0	1,492.3
2,500.0	1,500.5	2,500.0	1,500.5
3,000.0	1,509.3	3,000.0	1,509.3
3,011.0	1,509.5	3,011.0	1,509.5

Appendix Table 6 Weather and sea-state data

Monthly frequency distribution of wind direction in 1995

W.D / Month	CALM	N	NNE	NE	ENE	E	ESE	SE	SSE	S	SSW	SW	WSW	W	WNW	NW	NNW	Not Clear	Total
July %		12 2.51	44 9.17	39 8.13	60 12.50	46 9.59	76 15.83	71 14.79	34 7.08	21 4.37	12 2.51	11 2.29	10 2.08		2 0.42	9 1.88	33 6.87		480 100
August %		1 0.14		3 0.42	37 5.22	62 8.75	167 23.55	233 32.86	90 12.70	20 2.82								96 13.54	709 100

Monthly frequency distribution of wind velocity in 1995

(W.V : m/sec)

W.V / Month	CALM	1	2	3	4	5	6	7	8	9	10	11	12	13	14	15	16	17	Not Clear	Total
July %			10 2.08	34 7.08	45 9.38	75 15.62	71 14.79	87 18.12	62 12.93	50 10.42	13 2.70	11 2.29	17 3.54	3 0.63	1 0.21	1 0.21				480 100
August %		1 0.14	3 0.42	7 0.99	22 3.10	30 4.23	48 6.77	72 10.16	83 11.71	109 15.37	101 14.24	68 9.59	27 3.81	16 2.26	11 1.55	8 1.13	5 0.71	2 0.28	96 13.54	709 100

Monthly frequency distribution of weather in 1995

Weater / Month	Fine	Cloudy	Rain	Not clear	Total	Light rain
July %	14 70.00	5 25.00	1 5.00		20 100	4 20.00
August %	17 58.62	7 24.14		5 17.24	29 100	4 13.79

Monthly frequency distribution of atomospheric pressure (daily average) in 1995

(AP : hPa)

A.P / Month	1006.0 ～ 1006.9	1007.0 ～ 1007.9	1008.0 ～ 1008.9	1009.0 ～ 1009.9	1010.0 ～ 1010.9	1011.0 ～ 1011.9	1012.0 ～ 1012.9	1013.0 ～ 1013.9	1014.0 ～ 1014.9	1015.0 ～ 1015.9	1016.0 ～ 1016.9	1017.0 ～ 1017.9	1018.0 ～ 1018.9	1019.0 ～ 1019.9	1020.0 ～ 1020.9	1021.0 ～ 1021.9	1022.0 ～ 1022.9
July %	4 0.83	10 2.08	15 3.13	19 3.96	29 6.04	35 7.29	30 6.25	37 7.71	46 9.59	71 14.79	87 18.13	77 16.04	16 3.33	4 0.83			
August %							8 1.13	36 5.08	76 10.72	125 17.64	115 16.22	75 10.58	54 7.62	34 4.80	28 3.94	24 3.38	23 3.24

A.P / Month	1023.0 ～ 1023.9	1024.0 ～ 1024.9	Not Clear	Total
July %				480 100
August %	14 1.97	2 0.28	95 13.40	709 100

Monthly frequency distribution of swell height in 1995

S.D / Month	N	NNE	NE	ENE	E	ESE	SE	SSE	S	SSW	SW	WSW	W	WNW	NW	NNW	Not Clear	Total
July %	3 0.63		41 8.54	21 4.38	13 2.70	8 1.67	3 0.63	5 1.04	12 2.50	21 4.37	84 17.5	5 1.04		1 0.21	3 0.63		260 54.16	480 100
August %				2 0.28	11 1.55	46 6.49	122 17.21	49 6.91	47 6.63	1 0.14	4 0.56						427 60.23	709 100

Monthly frequency distribution of swell direction in 1995

(S.C : sec)

S.C / Month	3	4	5	6	7	8	9	10	11	12	13	Not Clear	Total
July %	1 0.21	2 0.42	9 1.88	42 8.75	48 10.00	25 5.22	71 14.79	21 4.37	1 0.21			260 54.16	480 100
August %		2 0.28	16 2.26	28 3.94	84 11.85	92 12.98	34 4.80	13 1.83		10 1.41	3 0.42	427 60.23	709 100

Monthly frequency distribution of swell cycle in 1995

(S.H : m)

S.H / Month	1	2	3	4	5	6	Not Clear	Total
July %	117 24.38	71 14.79	25 5.21	7 1.46			260 54.16	480 100
August %	37 5.22	126 17.77	82 11.57	22 3.10	11 1.55	4 0.56	427 60.23	709 100

Monthly frequency distribution of degree of cloudiness in 1995

D.C / Month	1	2	3	4	5	6	7	8	9	Not Clear	Total
July %	5 1.04	20 4.17	99 20.62	89 18.54	74 15.42	52 10.83	62 12.92	79 16.46			480 100
August %		10 1.41	115 16.22	140 19.75	131 18.48	81 11.42	37 5.22	100 14.10		95 13.40	709 100

[APPENDIX]

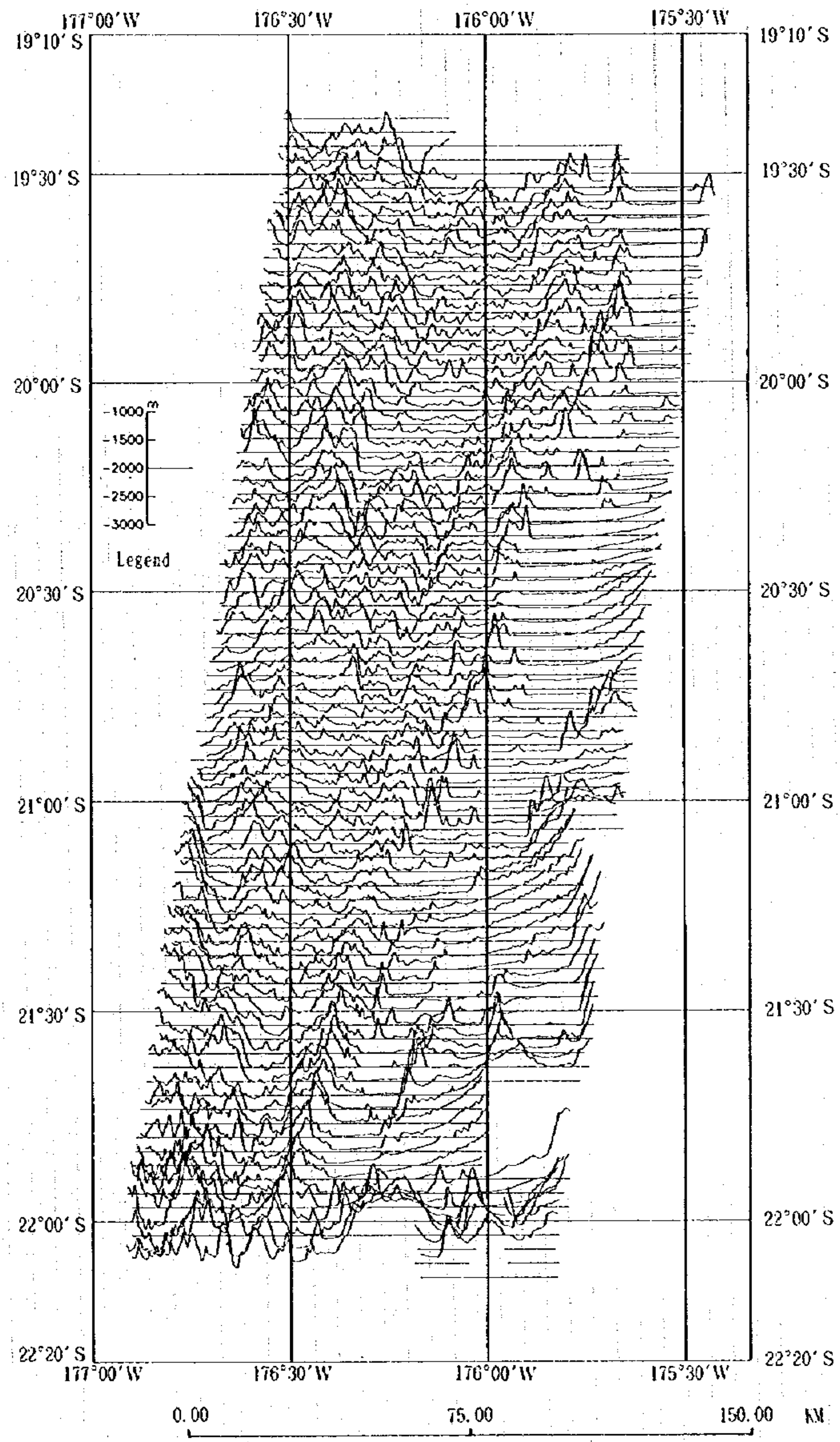

Appendix Fig. 1　Bathymetric profiles (all lines)

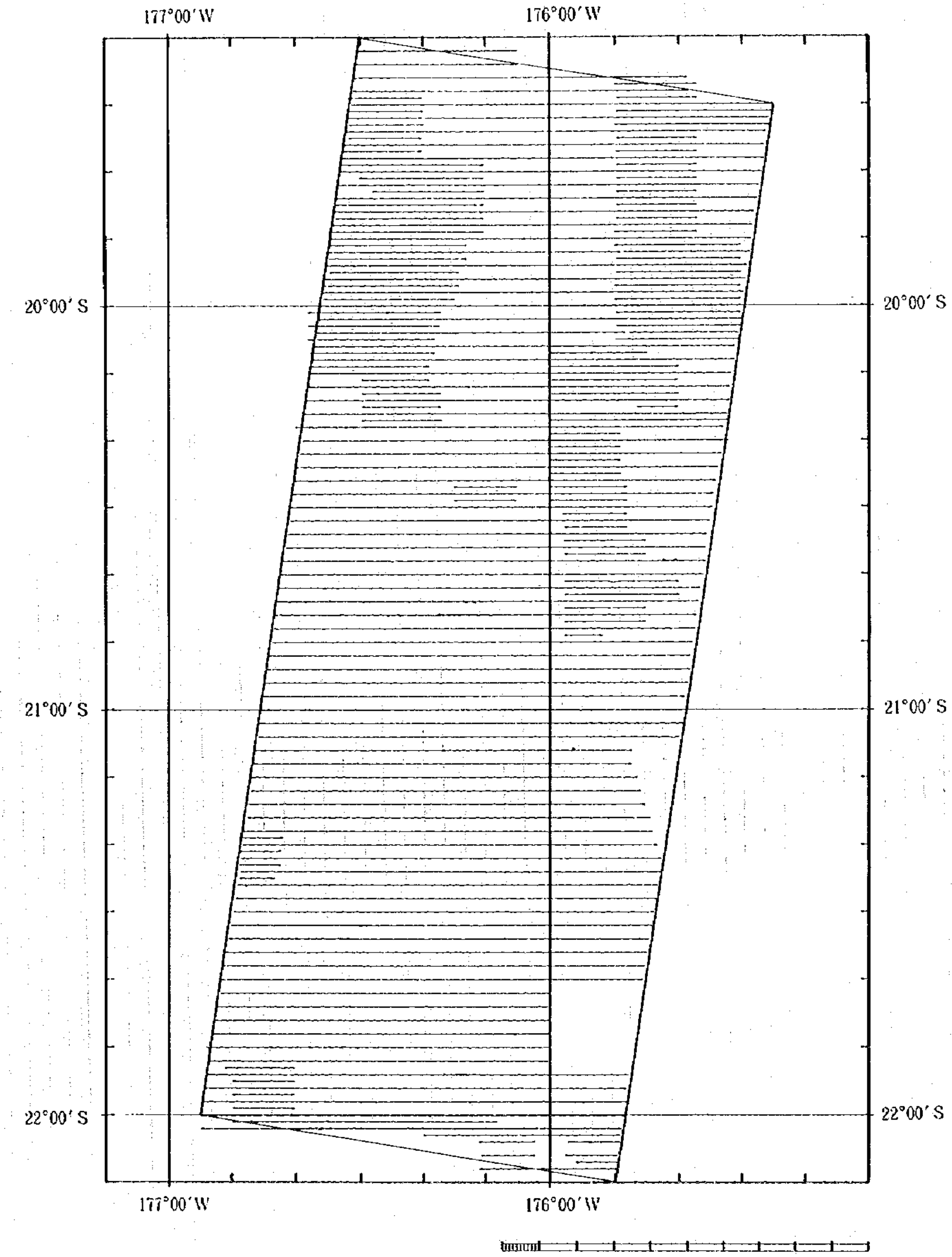

Appendix Fig. 2 MBES Track line map

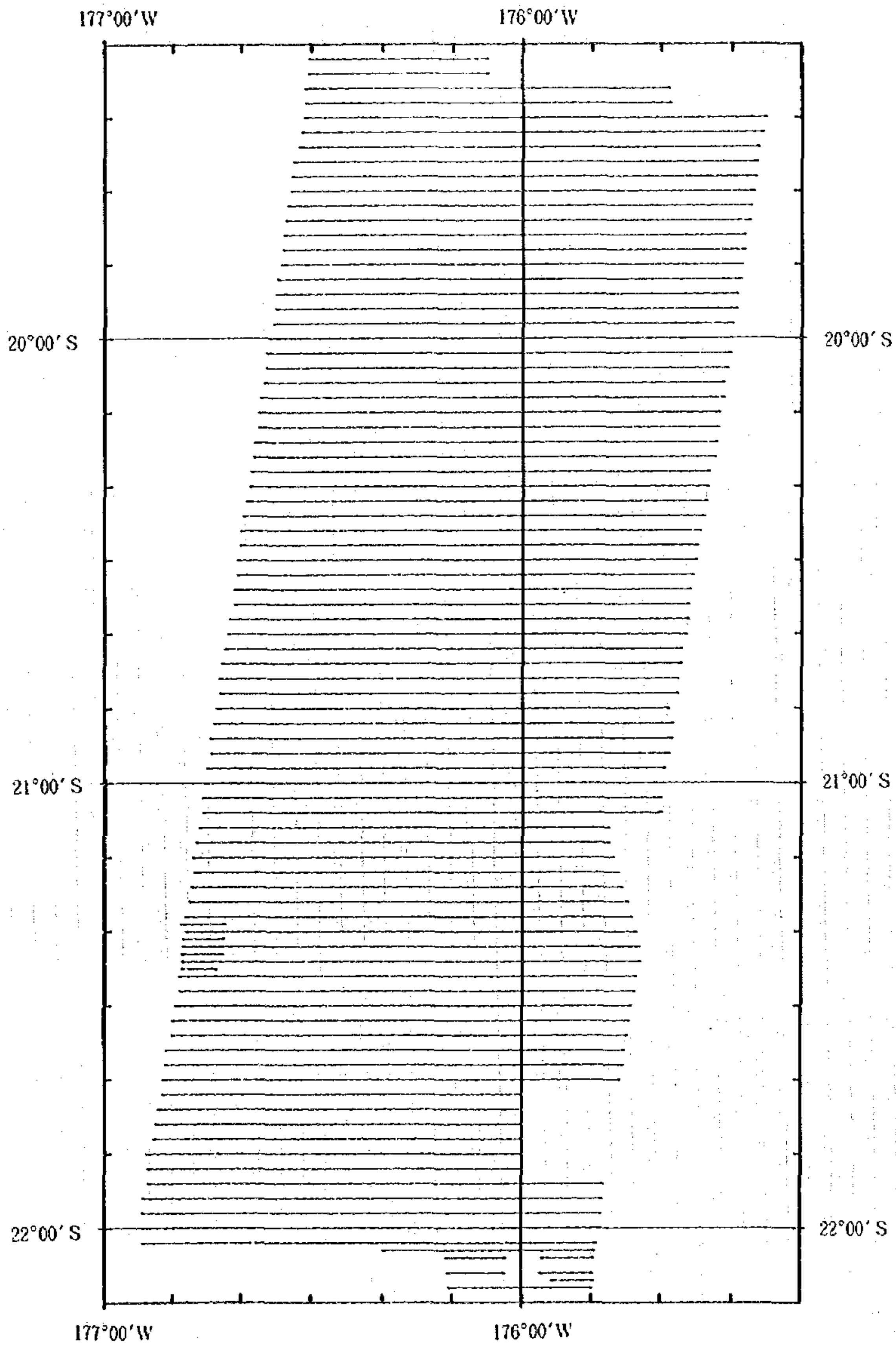

Appendix Fig. 3　PGM Track line map

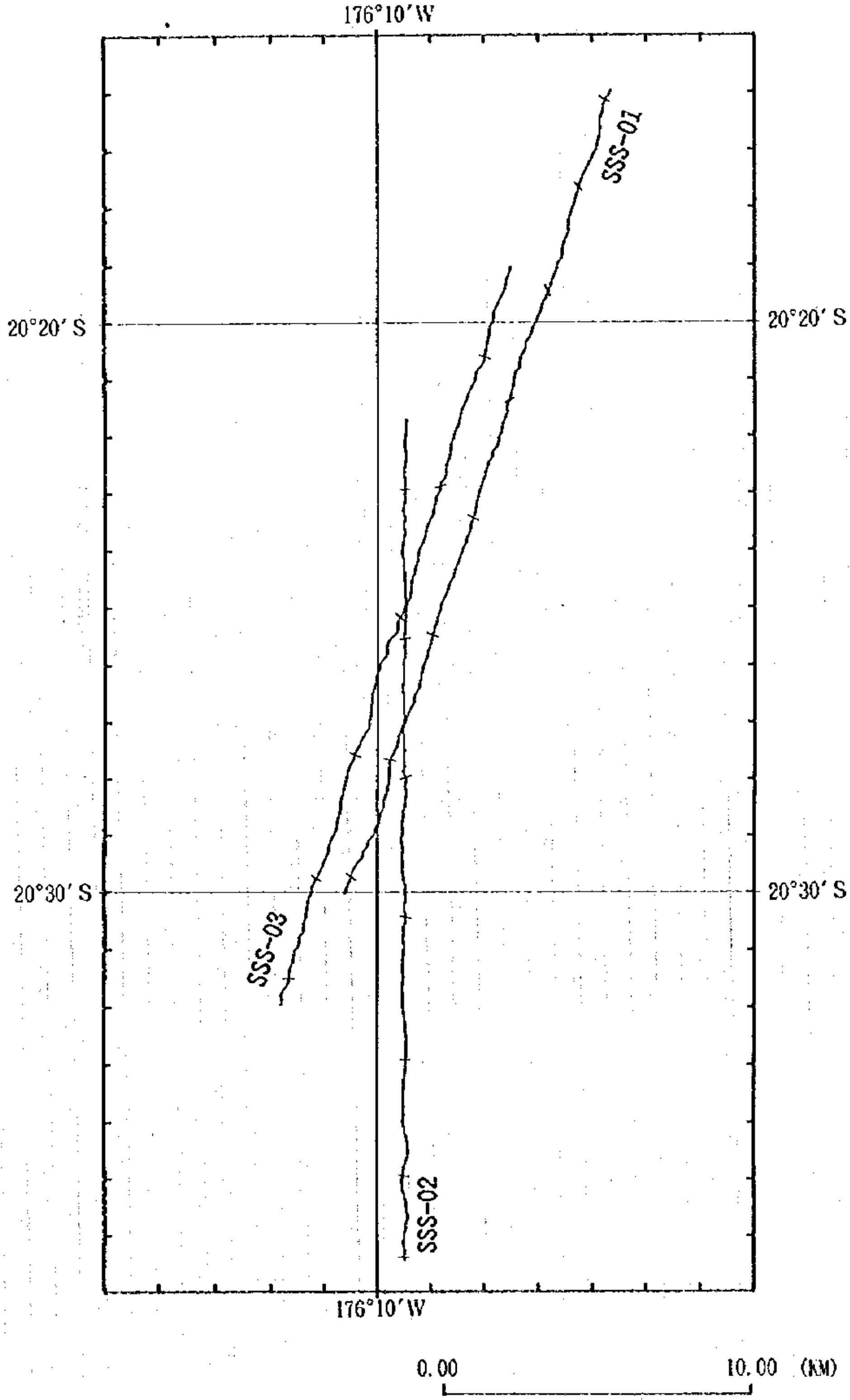

Appendix Fig. 4 SSS Vehicle position map

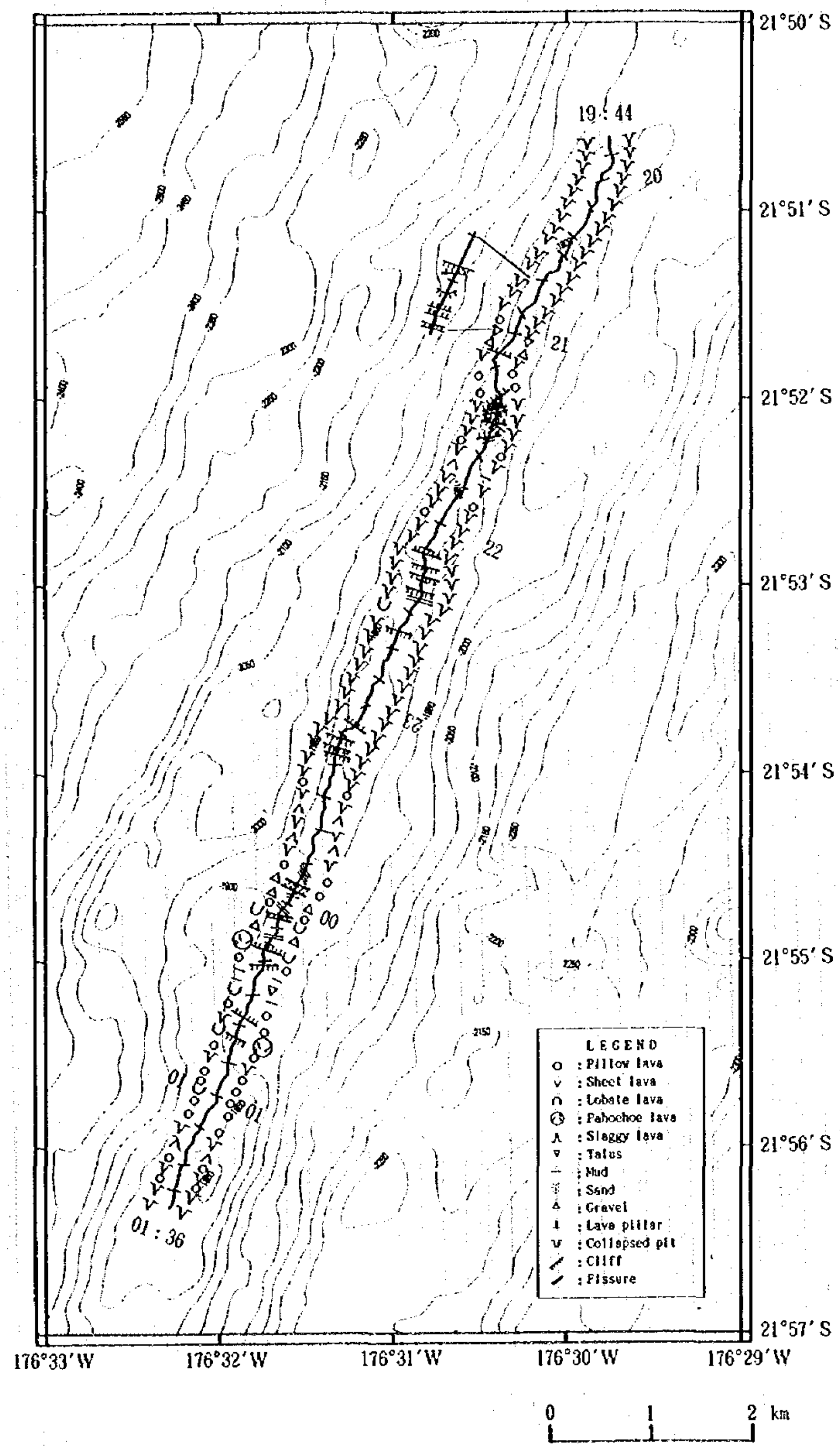

Appendix Fig.5 (1) Route-maps of FDC observation (95SFDC01)

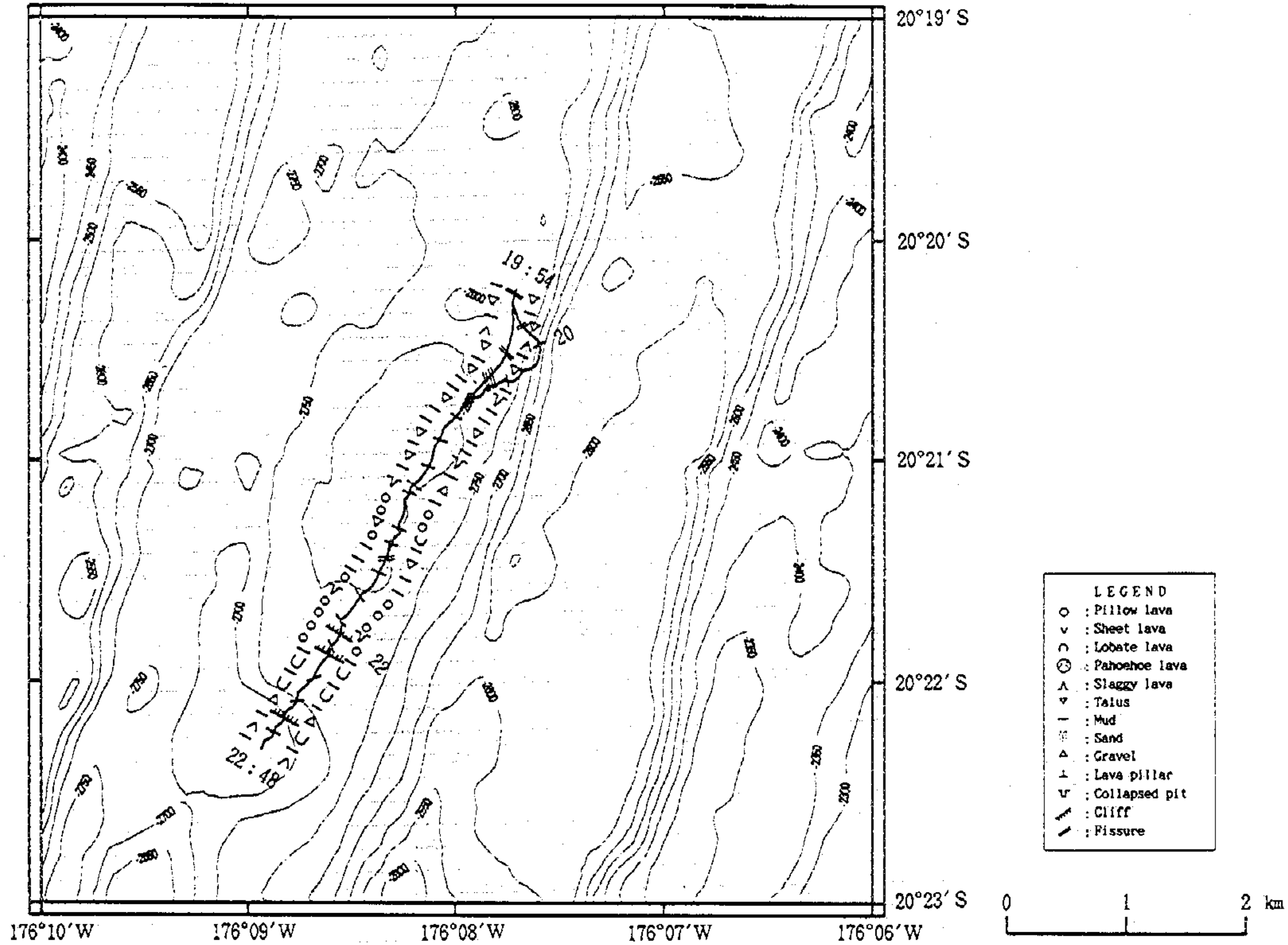

Appendix Fig.5 (2) Route-maps of FDC observation (95SFDC02)

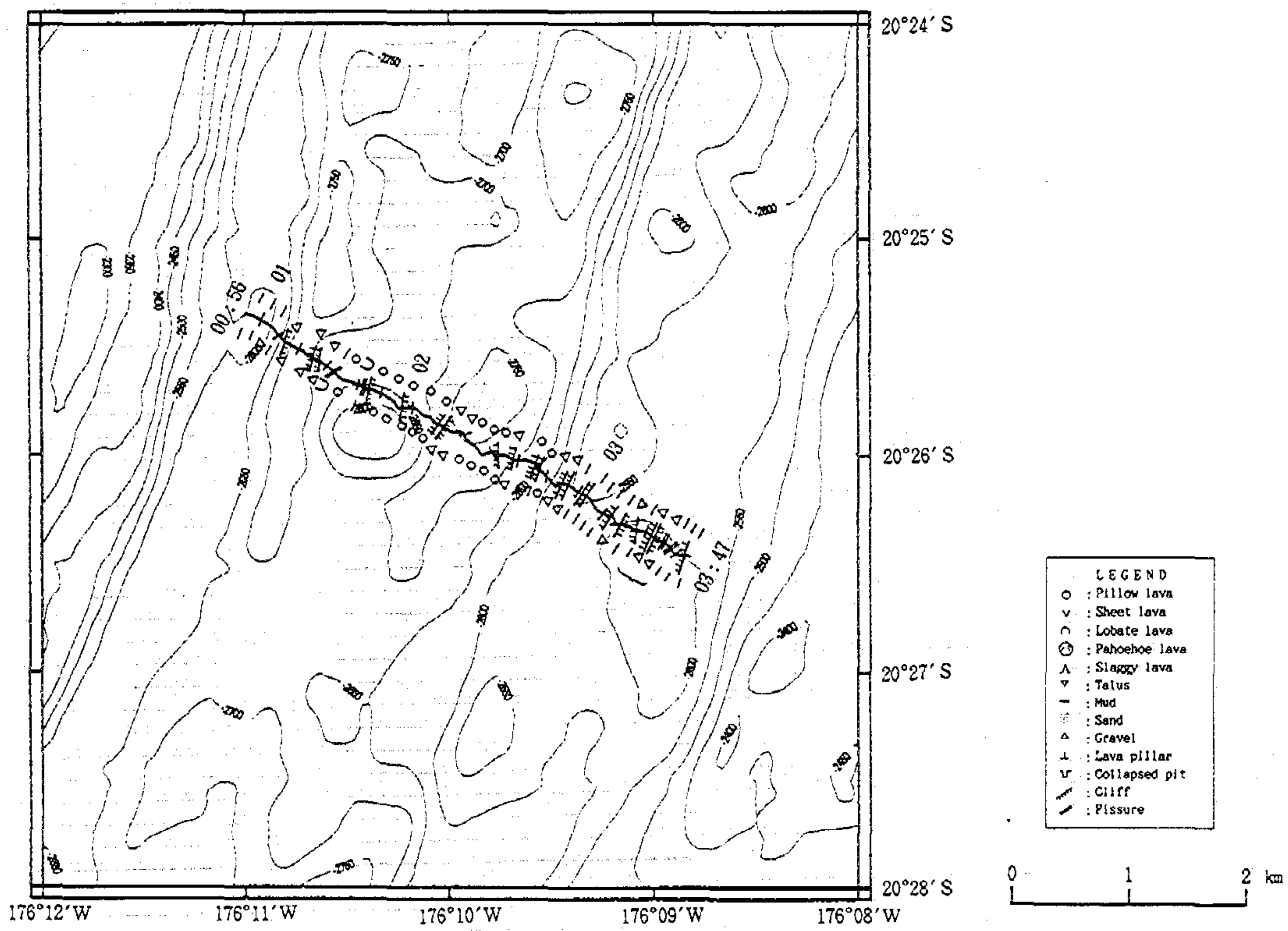

Appendix Fig.5 (3) Route-maps of FDC observation (95SFDC03)

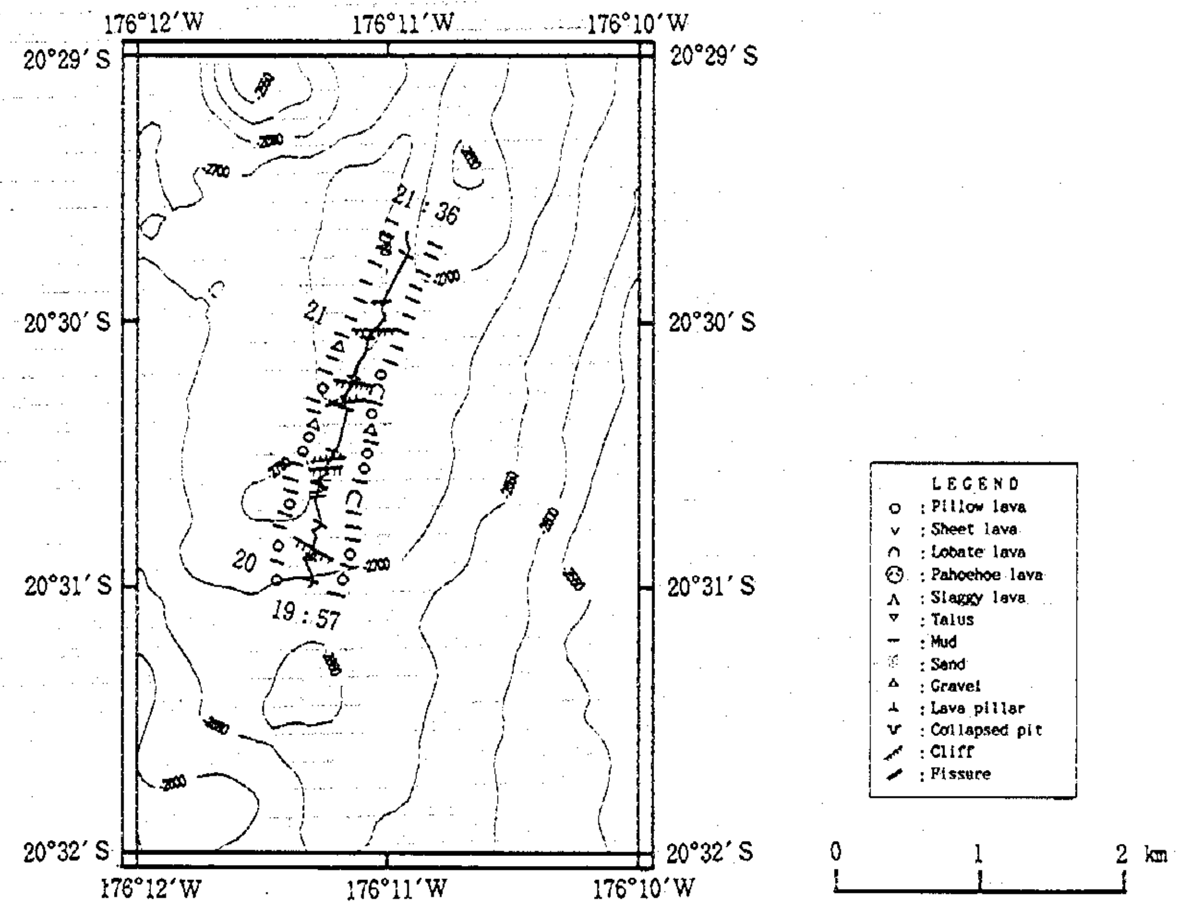

Appendix Fig.5 (4) Route-maps of FDC observation (95SFDC04)

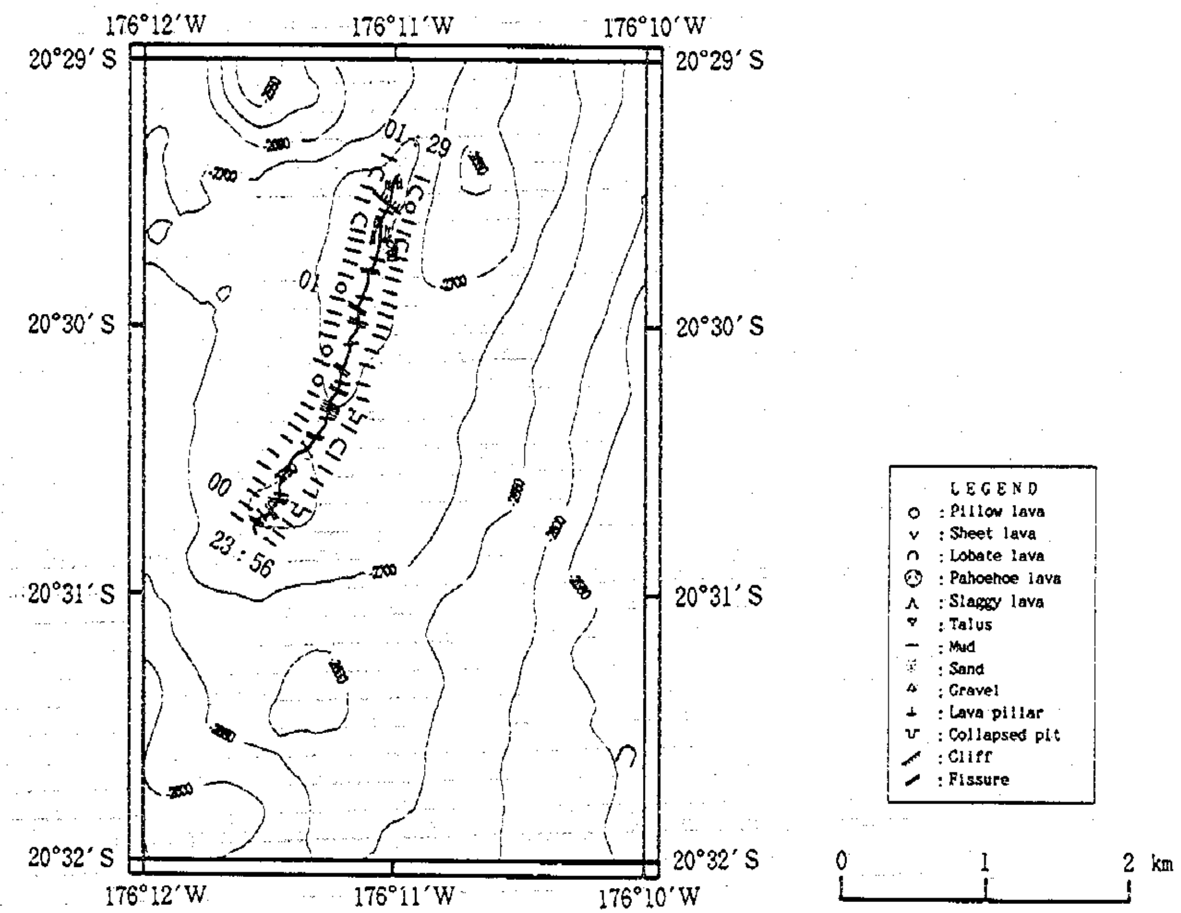

Appendix Fig.5 (5) Route-maps of FDC observation (95SFDC05)

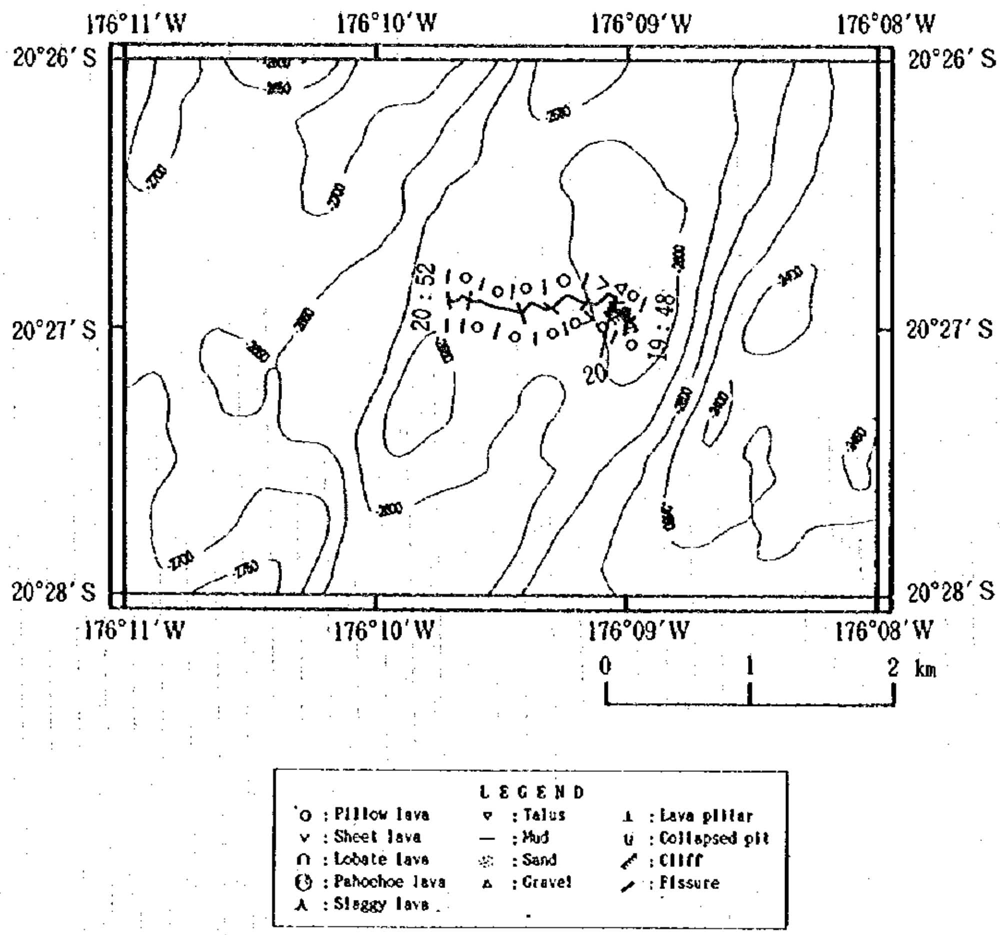

Appendix Fig.5 (6)   Route-maps of FDC observation (95SFDC06)

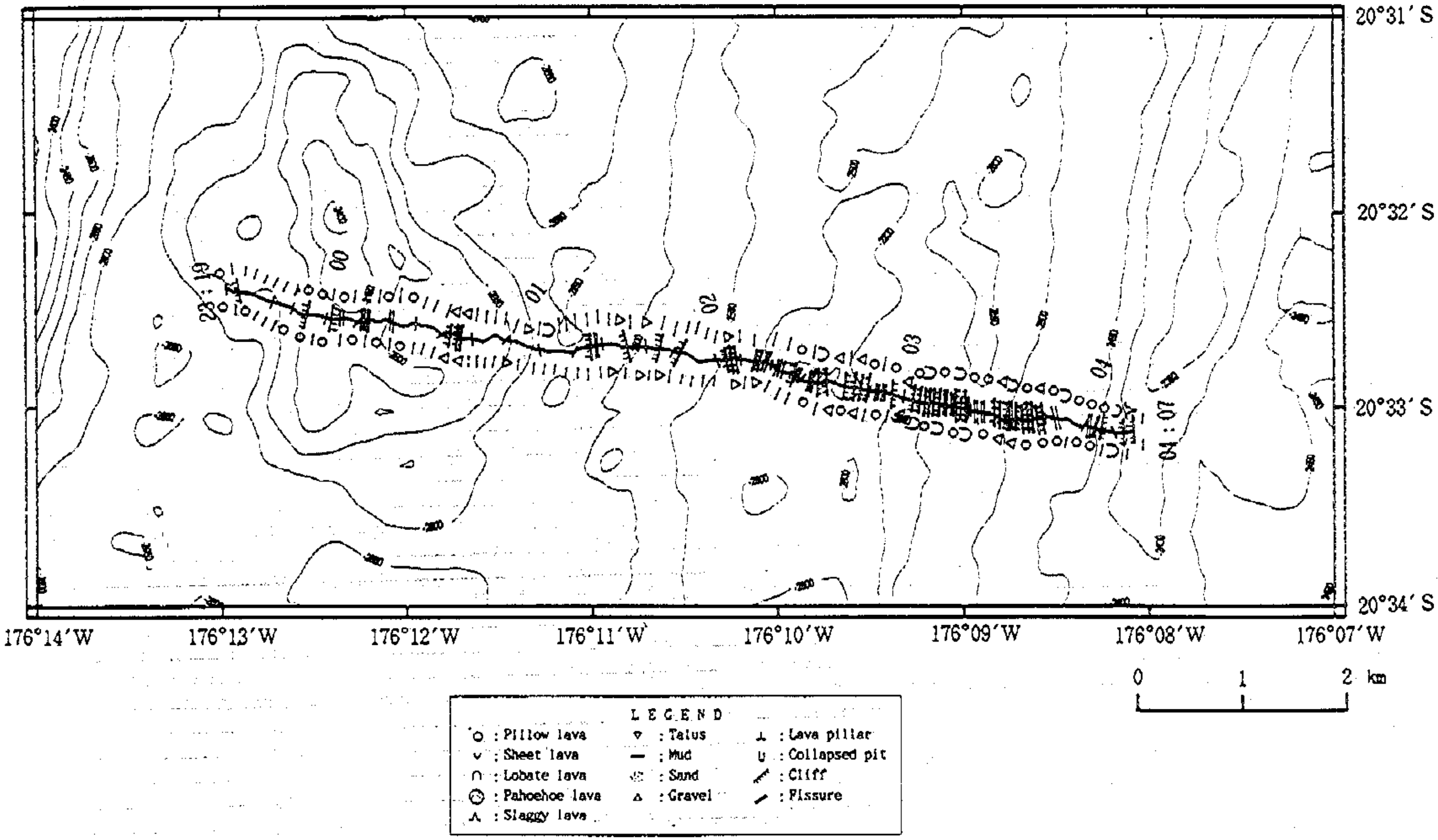

Appendix Fig.5 (7) Route-maps of FDC observation (95SFDC07)

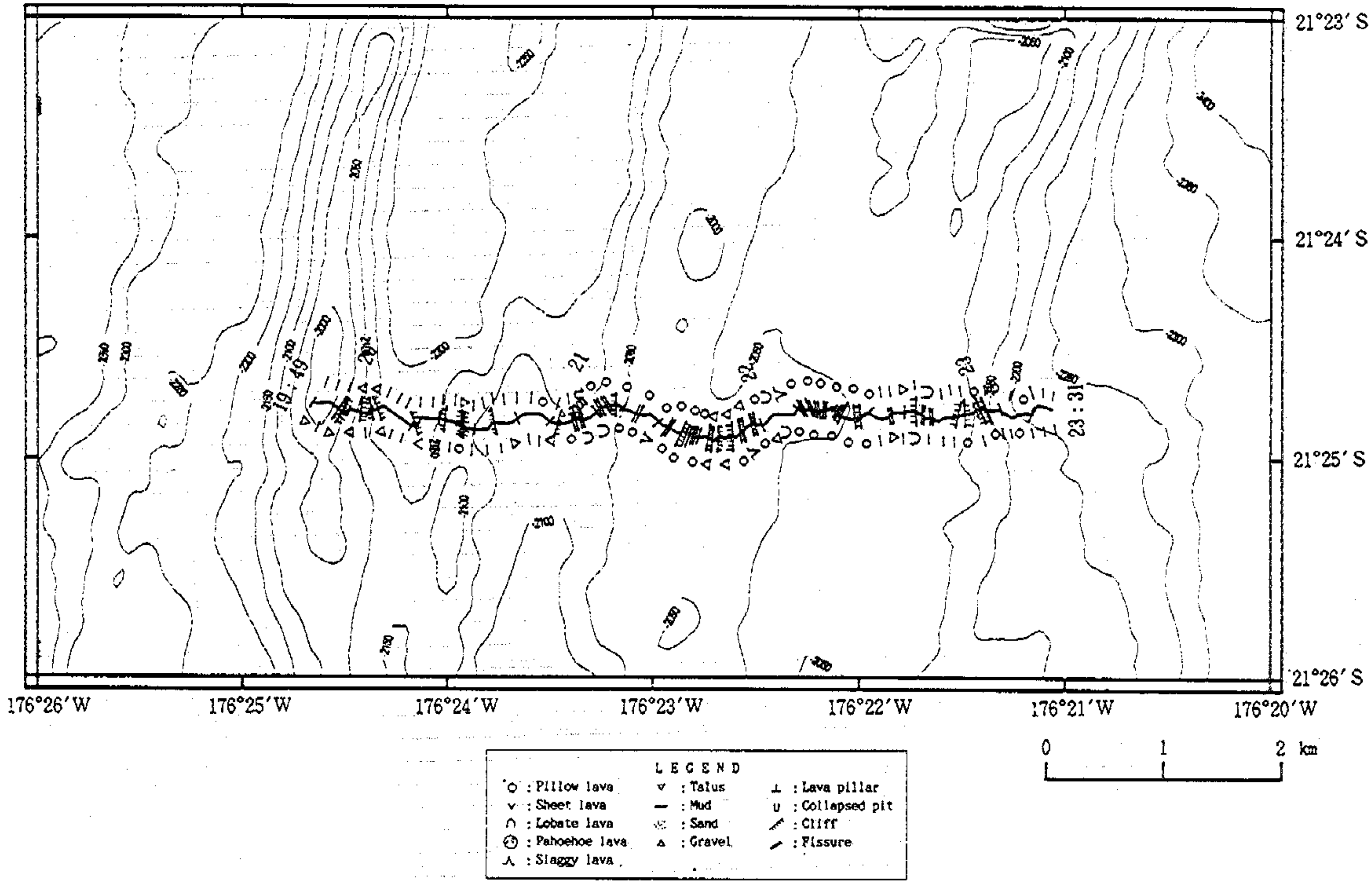

Appendix Fig.5 (8) Route-maps of FDC observation (95SFDC08)

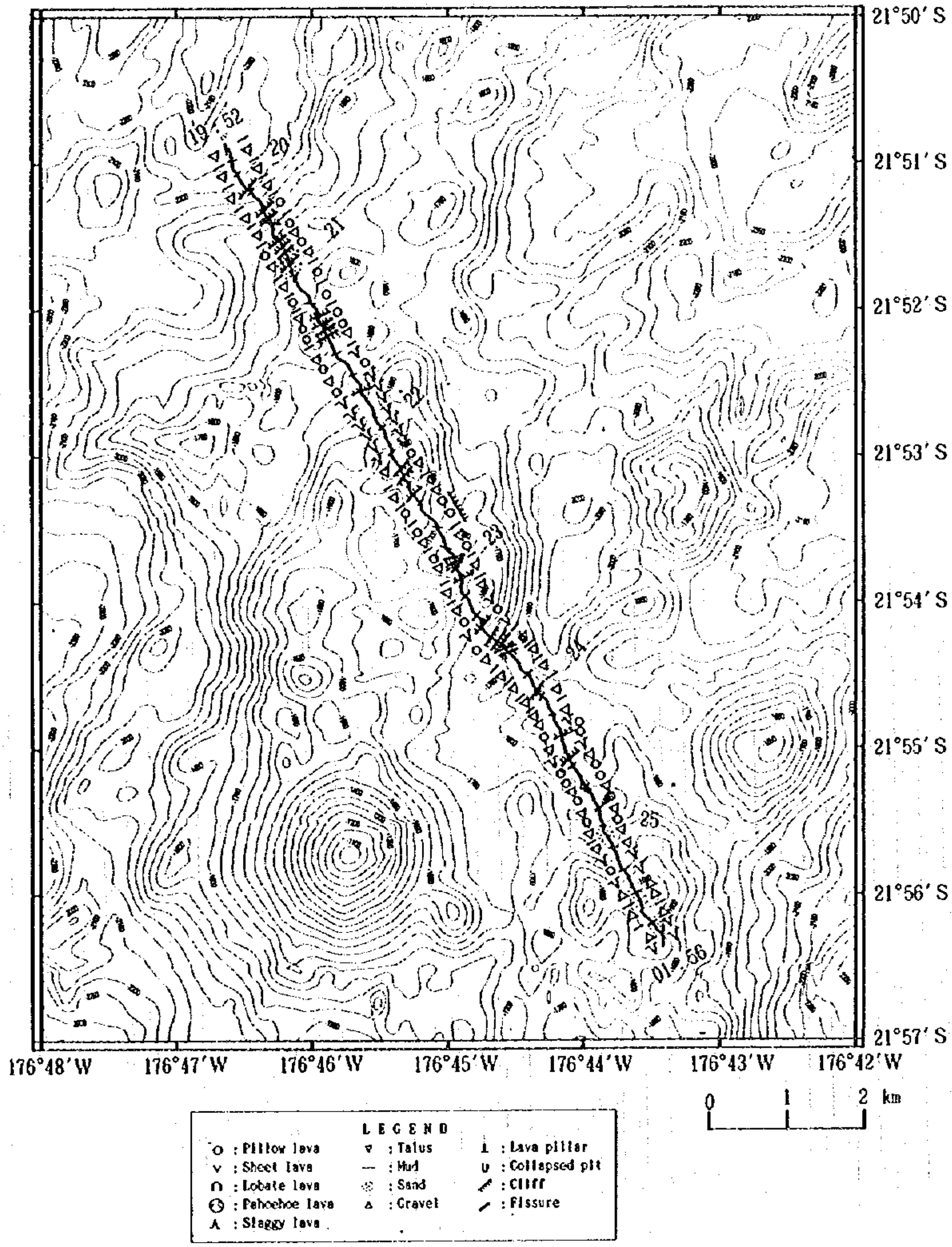

Appendix Fig.5 (9) Route-maps of FDC observation (95SFDC09)

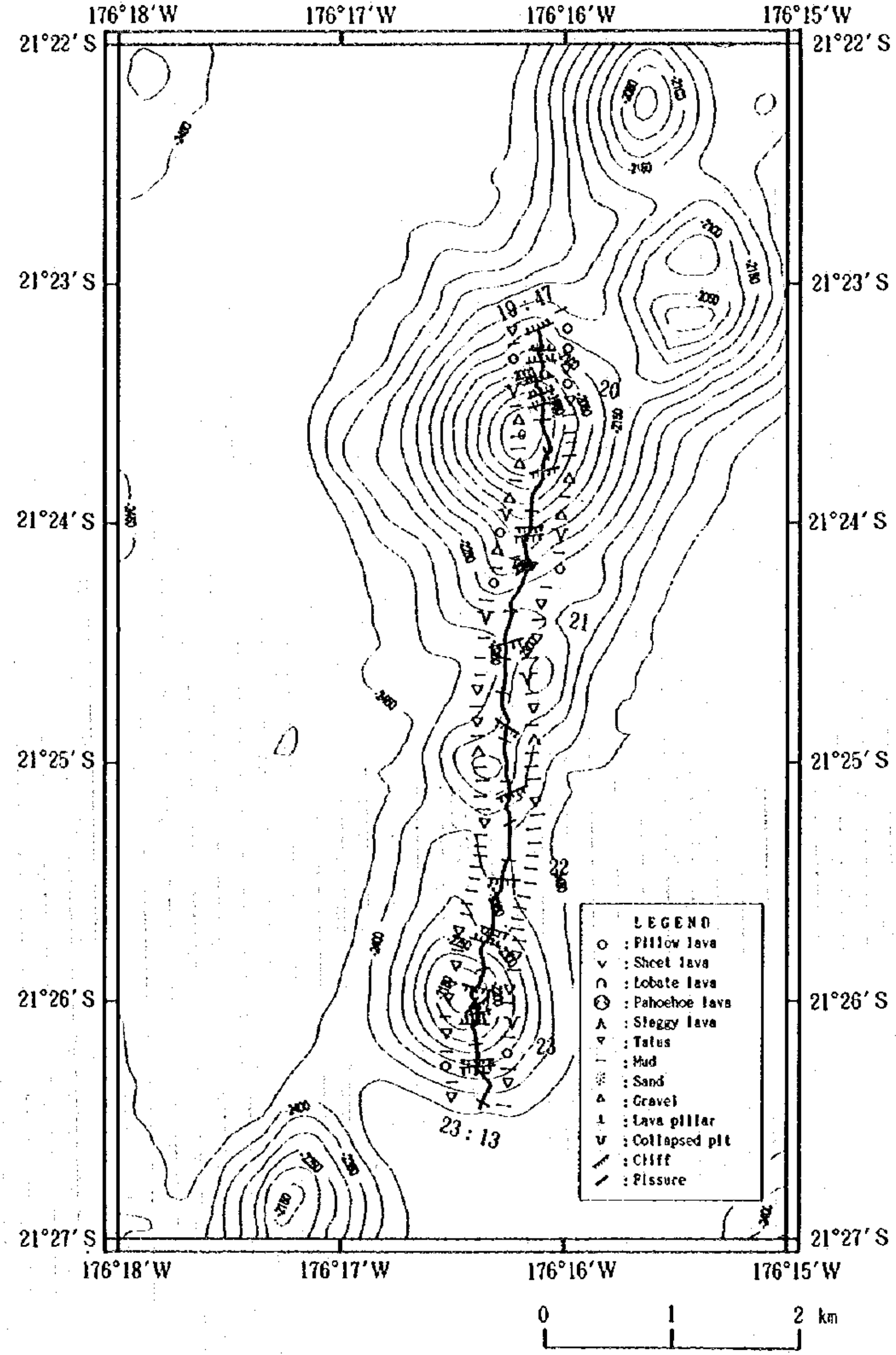

Appendix Fig.5 (10) Route-maps of FDC observation (95SFDC10)

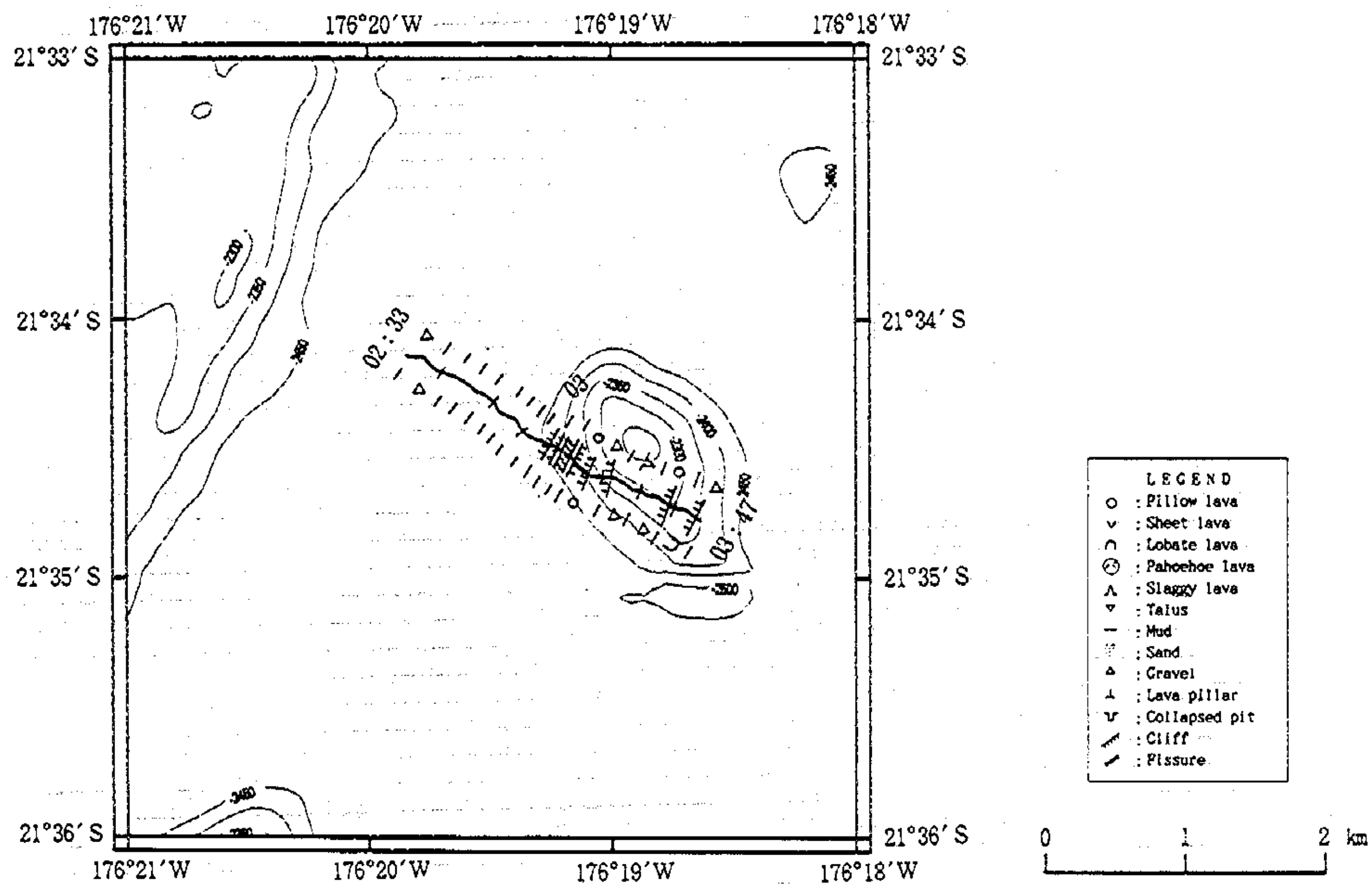

Appendix Fig.5 (11) Route-maps of FDC observation (95SFDC11)

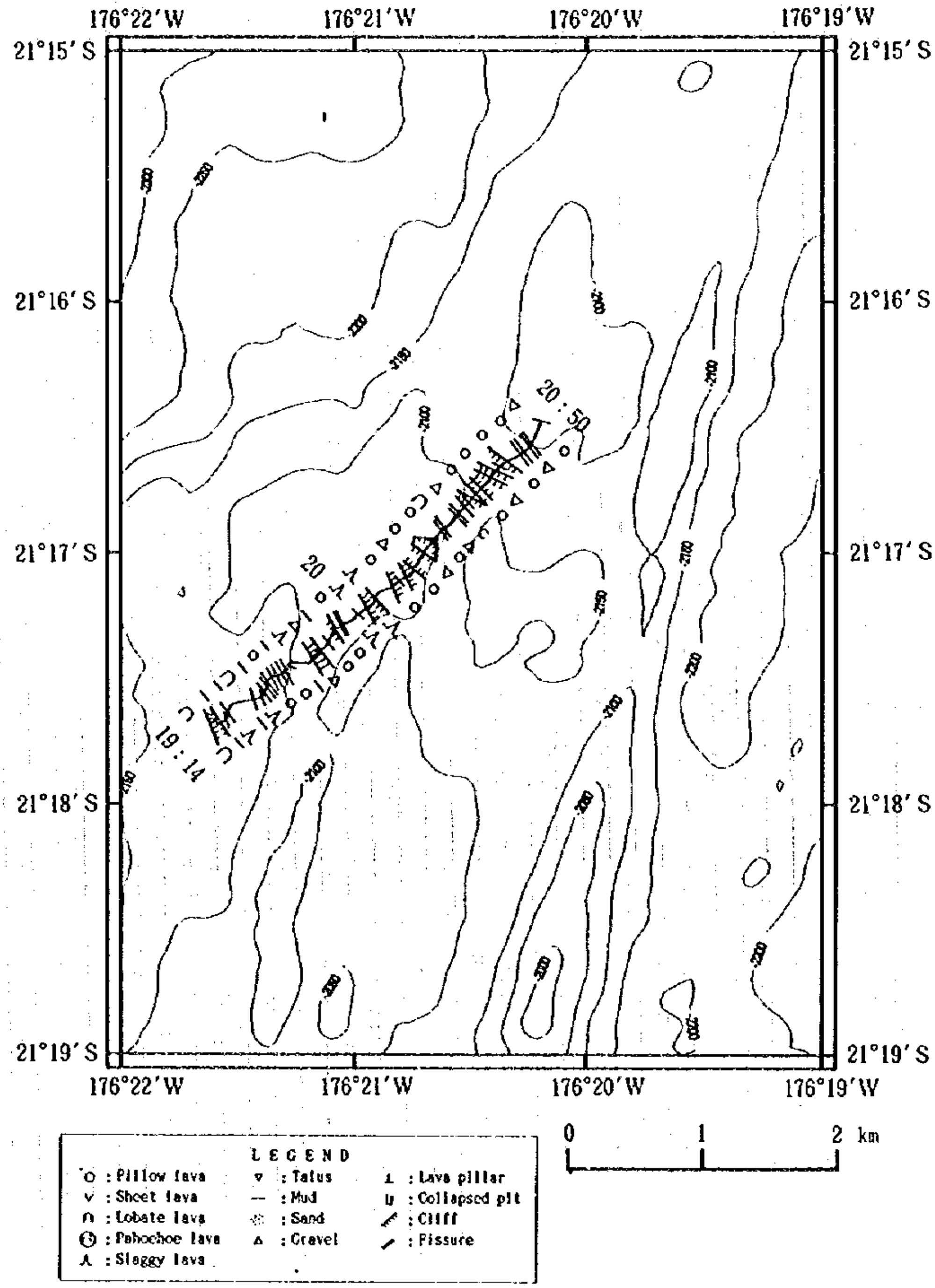

Appendix Fig.5 (12) Route-maps of FDC observation (95SFDC12)

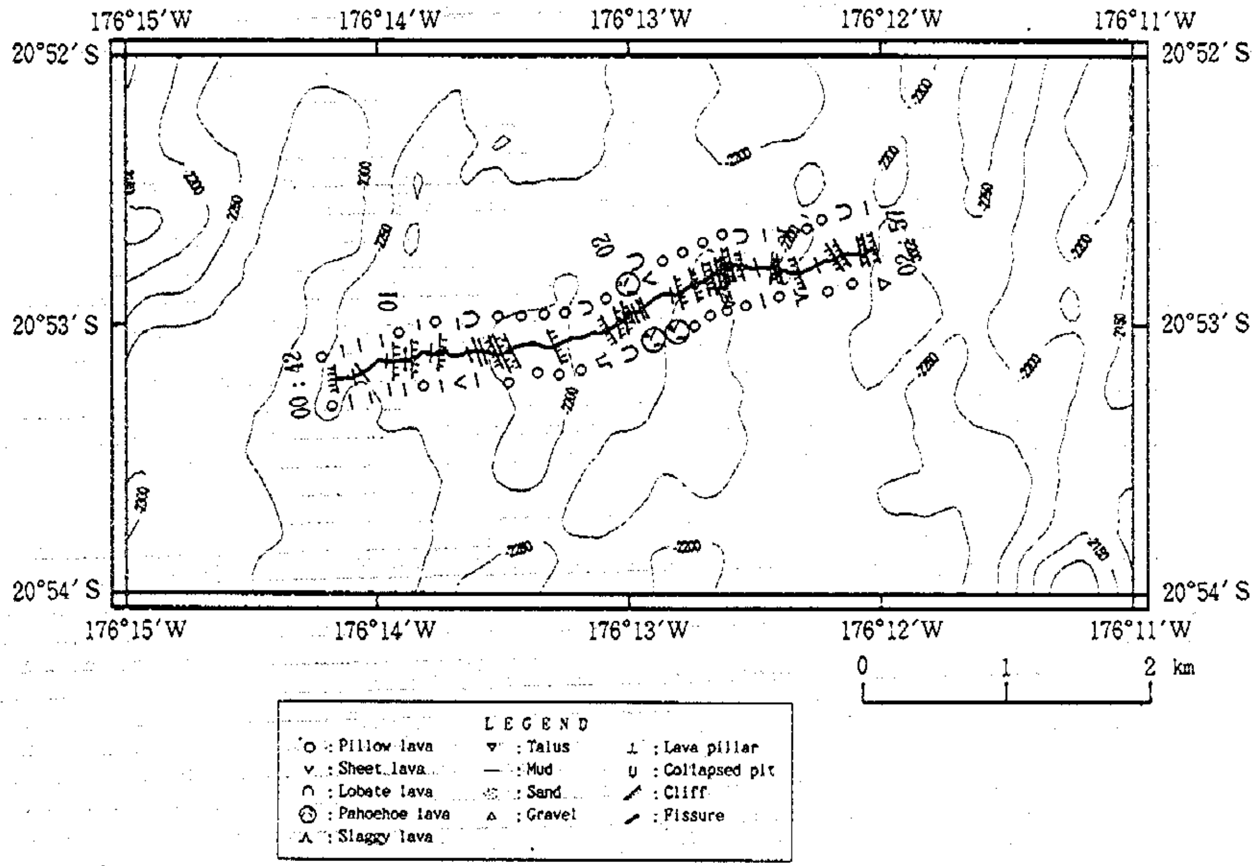

Appendix Fig.5 (13)   Route-maps of FDC observation (95SFDC13)

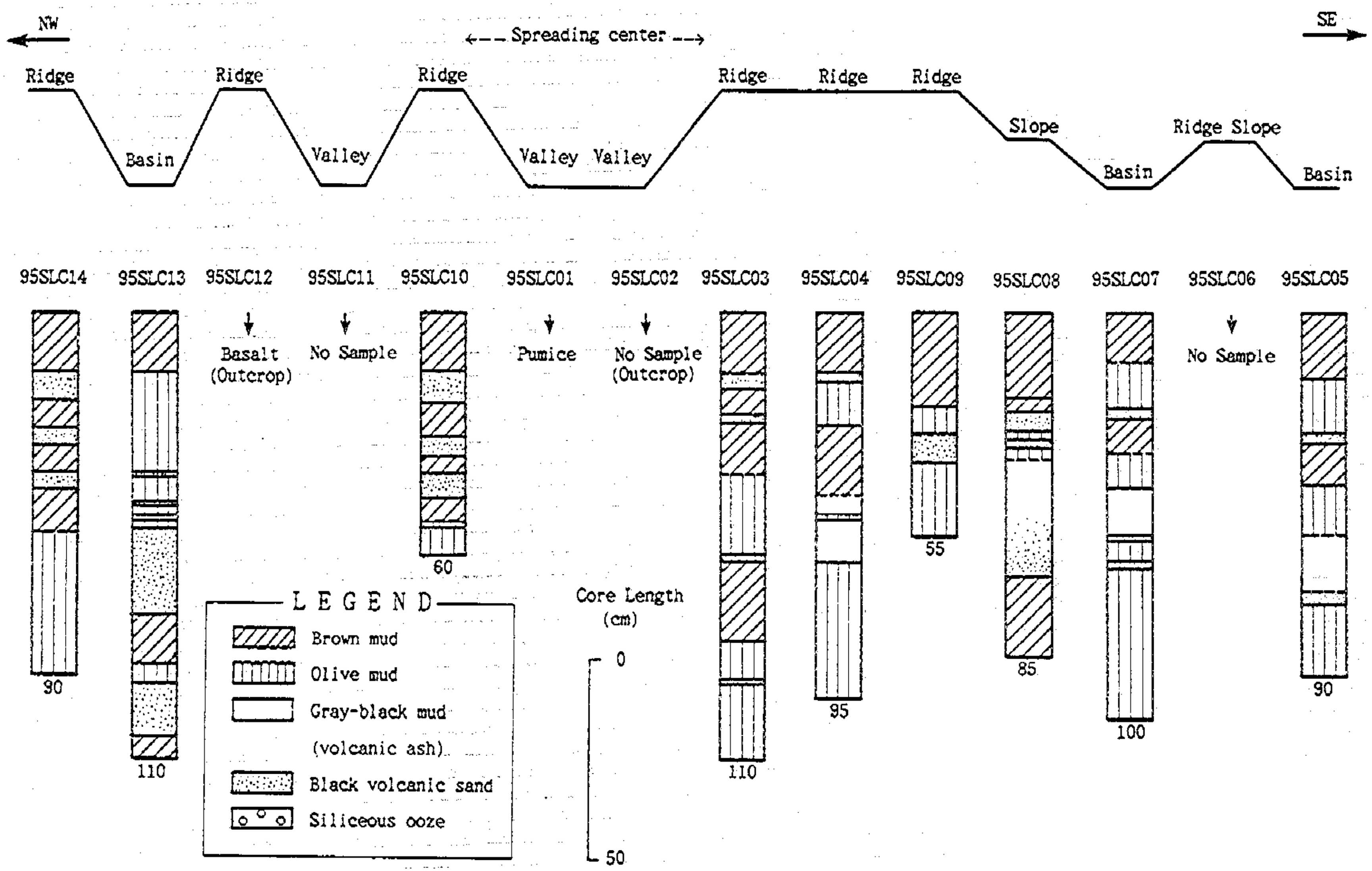

Appendix Fig. 6 (1) Columnar charts of LC core

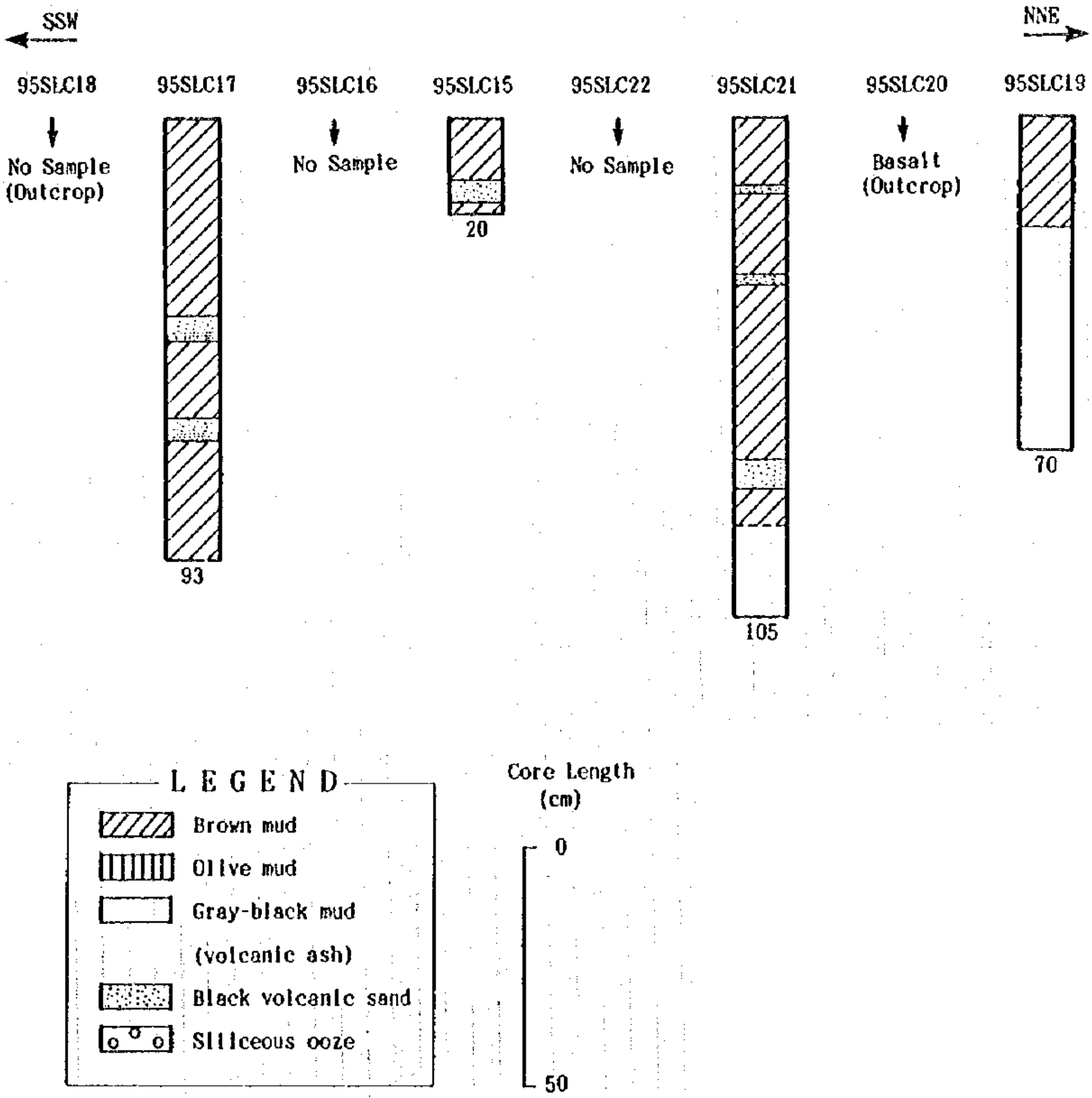

Appendix Fig. 6 (2) Columnar charts of LC core

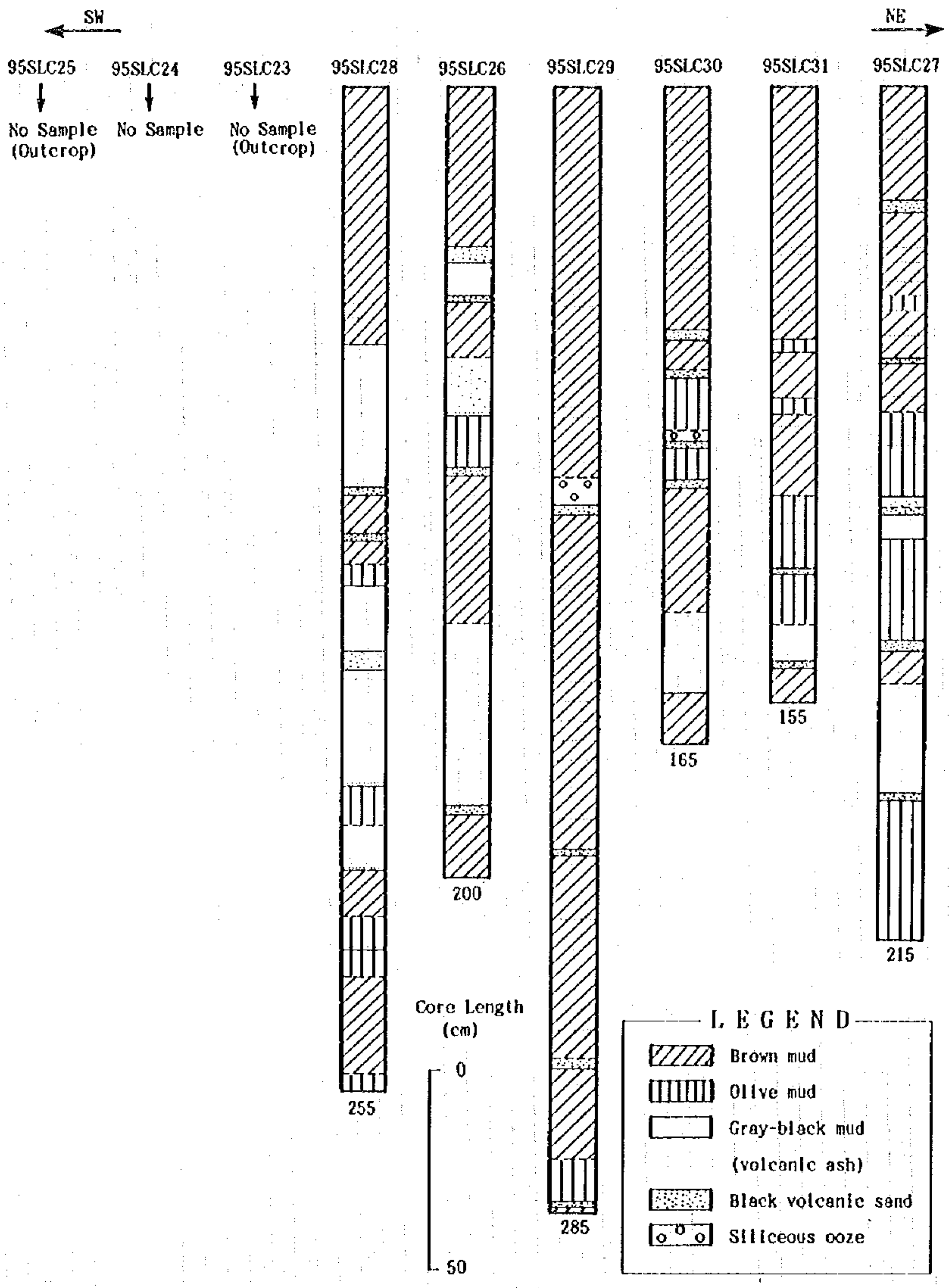

Appendix Fig. 6 (3) Columnar charts of LC core

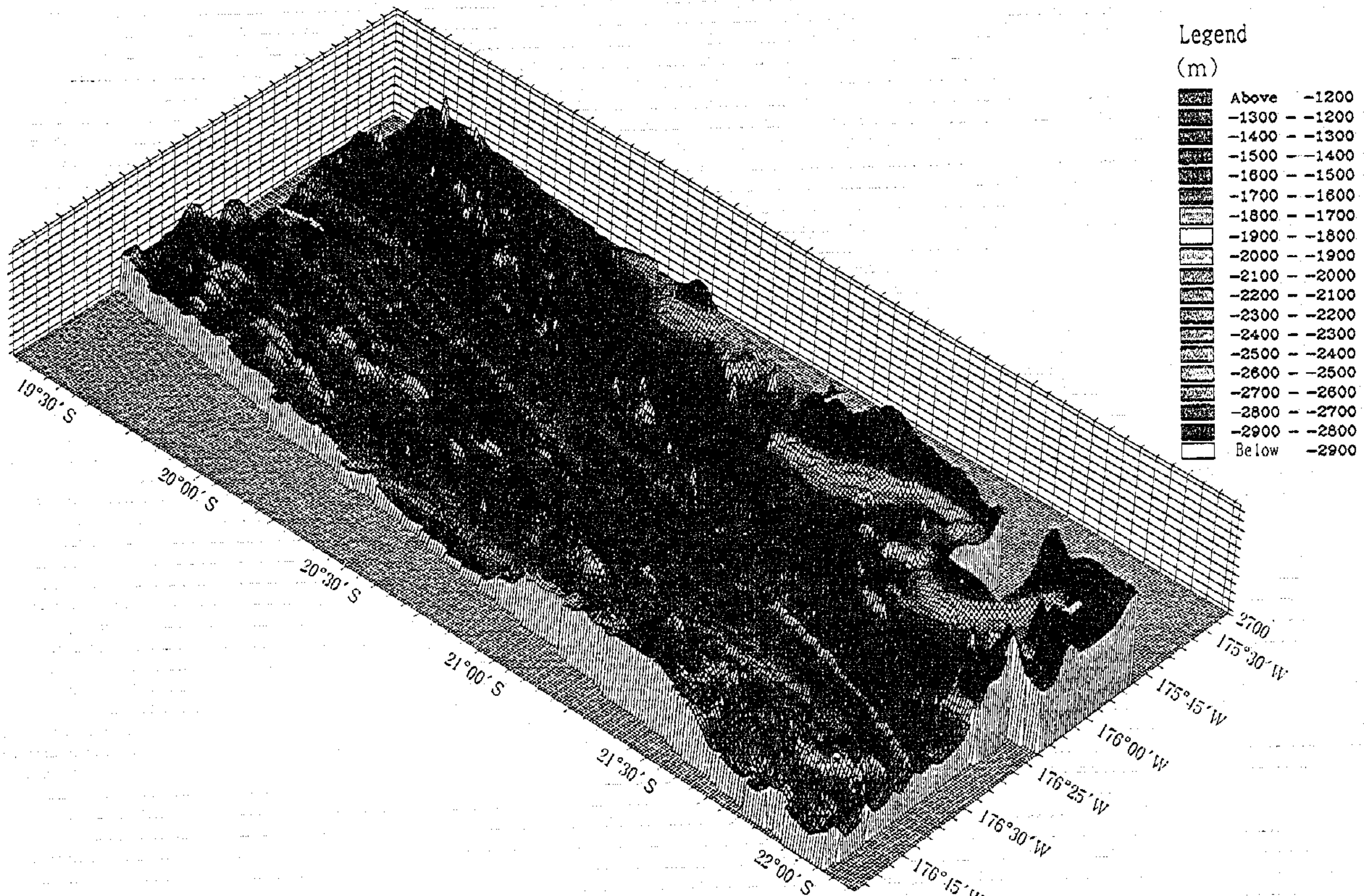

Appendix Fig. 7 3-D bathymetric map based on MBES.
Color change is every 100m.

JICA